TECHNICAL MEMORANDUM
X-297

INVESTIGATION OF THE LOW-SUBSONIC STABILITY AND CONTROL

CHARACTERISTICS OF A 1/3-SCALE FREE-FLYING MODEL OF

A LIFTING-BODY REENTRY CONFIGURATION

By James L. Hassell, Jr.

Langley Research Center
Langley Field, Va.

NATIONAL AERONAUTICS AND SPACE ADMINISTRATION

WASHINGTON   July 1960

Code-1

Copy # 1

NATIONAL AERONAUTICS AND SPACE ADMINISTRATION

TECHNICAL MEMORANDUM X-297

INVESTIGATION OF THE LOW-SUBSONIC STABILITY AND CONTROL

CHARACTERISTICS OF A 1/3-SCALE FREE-FLYING MODEL OF

A LIFTING-BODY REENTRY CONFIGURATION*

By James L. Hassell, Jr.

SUMMARY

An investigation of the low-subsonic stability and control characteristics of a 1/3-scale free-flying model of a rounded half-cone lifting-body reentry configuration has been made in the Langley full-scale tunnel. The static longitudinal and lateral stability characteristics were satisfactory and the damping of the Dutch roll oscillation was good for all flight conditions tested. Although the lower pair of control surfaces employed as elevators provided a rather weak pitch control, this deficiency presented no particular problem in these tests since no abrupt changes occurred in trim or stability. The lateral control effectiveness decreased with increase in angle of attack and increased as the neutral setting of the upper pair of surfaces employed as ailerons was moved trailing-edge upward. Adequate lateral control could be obtained for angles of attack up to about 33° if the ailerons were initially trimmed about 40° trailing edge up.

INTRODUCTION

As a part of an overall research program being conducted by the National Aeronautics and Space Administration on possible reentry configurations, tests of a 1/3-scale lifting-body reentry vehicle have been made for the purpose of evaluating the dynamic stability and control characteristics for the subsonic phase of the flight.

It has been pointed out in reference 1 that one advantage of the nonlifting blunt-body type of reentry vehicle is its ability to withstand severe aerodynamic heating over the relatively short period of

---

*Title, Unclassified.

time required for reentry into the atmosphere, but the high decelerations experienced during this short time interval pose somewhat of a problem for a vehicle intended for manned reentry. A ballistic missile nose cone modified to provide some lift has been proposed as a possible manned reentry vehicle because its lifting capability would appreciably reduce the high deceleration forces and at the same time its ability to withstand severe aerodynamic heating would be retained at least to some degree. A configuration based on this concept was derived by removing a portion of a blunted $60°$ apex angle cone to form a flat-topped body and rounding off the edges of this surface to reduce local heating. The choice of the $6.6°$ slope of the upper surface was purely arbitrary and was not dictated by aerodynamic considerations. The vehicle is equipped with reaction controls for use outside the dense atmosphere and two pairs of tablike surfaces for aerodynamic control upon reentry into the atmosphere. High Mach number data and some theoretical work on this configuration are available in reference 1 and other subsonic development work is presented in reference 2.

The present investigation included flight tests in the Langley full-scale tunnel to determine the low-subsonic flight characteristics of the model over an angle-of-attack range from $15°$ to $39°$ and force tests in the Langley free-flight tunnel to determine the static and dynamic stability and control characteristics over an angle-of-attack range from $0°$ to $90°$.

DEFINITION OF TERMS AND SYMBOLS

All longitudinal aerodynamic data are referred to the wind axes and the lateral aerodynamic data are referred to the body axes. (See fig. 1.) Both longitudinal and lateral data are referred to a moment center (corresponding to the center of gravity of the flight-test model) which is located 66 percent of the body length aft of the nose and 19 percent of the body length below the basic cone center line. (See fig. 2.) The term "in-phase derivative" used herein refers to any one of the stability derivatives which are based on the forces or moments in phase with the angle of roll, yaw, or sideslip produced in the oscillatory tests. The term "out-of-phase derivative" refers to any one of the stability derivatives which are based on the forces or moments $90°$ out of phase with the angle of roll, yaw, or sideslip. The derivatives measured in the investigation are summarized in table I. All measurements are reduced to standard coefficient form and are presented in terms of the following symbols:

b wing span (maximum lateral dimension of the body), ft

$C_{1/2}$ cycles to damp to half amplitude, $\dfrac{T_{1/2}}{P}$

C_D drag coefficient, $\dfrac{F_D}{qS}$

C_l rolling-moment coefficient, $\dfrac{M_X}{qSb}$

C_L lift coefficient, $\dfrac{F_L}{qS}$

C_m pitching-moment coefficient, $\dfrac{M_Y}{qSL}$

C_n yawing-moment coefficient, $\dfrac{M_Z}{qSb}$

C_Y side-force coefficient, $\dfrac{F_Y}{qS}$

f frequency of oscillation, cps

F_D drag, lb

F_L lift, lb

F_N normal force, lb

F_X axial force, lb

F_Y side force, lb

I_X moment of inertia about X body axis, slug-ft^2

I_{XZ} product of inertia, slug-ft^2

I_Y moment of inertia about Y body axis, slug-ft^2

I_Z moment of inertia about Z body axis, slug-ft^2

k reduced frequency parameter, $\dfrac{\omega b}{2V}$

k_X radius of gyration about X body axis, ft

k_Y radius of gyration about Y body axis, ft

k_Z	radius of gyration about Z body axis, ft
L	body length (excluding control surfaces), ft
L/D	lift-drag ratio
m	mass, slugs
M_X	rolling moment, ft-lb
M_Y	pitching moment, ft-lb
M_Z	yawing moment, ft-lb
p	rolling velocity, radians/sec
$\dot{p} = \dfrac{dp}{dt}$	
P	period, sec
q	free-stream dynamic pressure, lb/sq ft
r	yawing velocity, radians/sec
$\dot{r} = \dfrac{dr}{dt}$	
R	radius, in.
S	wing area (body plan-form area) $\left(S = 0.9L^2\right)$, sq ft
t	time, sec
$T_{1/2}$	time to damp to half-amplitude, sec
V	free-stream velocity, ft/sec
W	weight, lb
X,Y,Z	body reference axes unless otherwise noted
α	angle of attack, deg
β	angle of sideslip, deg or radians

$$\dot{\beta} = \frac{d\beta}{dt}$$

γ flight-path angle, positive for climb, deg

Δ used as coefficient prefix to indicate incremental value due to 20° differential control deflection of upper surfaces (corresponds to deflections of upper pair of surfaces used in flight tests)

δ_e elevator deflection (both lower surfaces deflected together), positive for trailing edges down, deg. Surfaces considered undeflected $\left(\delta_e = 0^\circ\right)$ when parallel with basic cone center line

ϵ angle between principal axis and X body axis (positive for principal axis nose down with respect to body axis), deg

μ_b relative density factor, $\dfrac{m}{\rho S b}$

ρ mass density of air, slugs/cu ft

ϕ angle of bank, deg

ψ angle of yaw, deg

$\omega = 2\pi f$, radians/sec

$$C_{l_\beta} = \frac{\partial C_l}{\partial \beta}, \text{ per radian,} \qquad C_{n_\beta} = \frac{\partial C_n}{\partial \beta}, \text{ per radian,} \qquad C_{Y_\beta} = \frac{\partial C_Y}{\partial \beta}, \text{ per radian}$$

$$C_{l_r} = \frac{\partial C_l}{\partial \frac{rb}{2V}}, \text{ per radian,} \qquad C_{n_r} = \frac{\partial C_n}{\partial \frac{rb}{2V}}, \text{ per radian,} \qquad C_{Y_r} = \frac{\partial C_Y}{\partial \frac{rb}{2V}}, \text{ per radian}$$

$$C_{l_p} = \frac{\partial C_l}{\partial \frac{pb}{2V}}, \text{ per radian,} \qquad C_{n_p} = \frac{\partial C_n}{\partial \frac{pb}{2V}}, \text{ per radian,} \qquad C_{Y_p} = \frac{\partial C_Y}{\partial \frac{pb}{2V}}, \text{ per radian}$$

$$C_{l_{\dot{\beta}}} = \frac{\partial C_l}{\partial \frac{\dot{\beta}b}{2V}}, \qquad C_{n_{\dot{\beta}}} = \frac{\partial C_n}{\partial \frac{\dot{\beta}b}{2V}}, \qquad C_{Y_{\dot{\beta}}} = \frac{\partial C_Y}{\partial \frac{\dot{\beta}b}{2V}}$$

$$C_{l_{\dot r}} = \frac{\partial C_l}{\partial \frac{\dot r b}{2V}^2}, \qquad C_{n_{\dot r}} = \frac{\partial C_n}{\partial \frac{\dot r b}{2V}^2}, \qquad C_{Y_{\dot r}} = \frac{\partial C_Y}{\partial \frac{\dot r b}{2V}^2}$$

$$C_{l_{\dot p}} = \frac{\partial C_l}{\partial \frac{\dot p b}{2V}^2}, \qquad C_{n_{\dot p}} = \frac{\partial C_n}{\partial \frac{\dot p b}{2V}^2}, \qquad C_{Y_{\dot p}} = \frac{\partial C_Y}{\partial \frac{\dot p b}{2V}^2}$$

MODEL AND APPARATUS

The model used in this investigation was built at the Langley Research Center. Basically, the model was constructed by fitting a thin molded fiberglass shell over a magnesium cruciform framework. This construction provided the relatively lightweight model required for the free-flight and oscillation test techniques employed in this investigation. The model was equipped with two pairs of control surfaces hinged at the base of the body. A three-view drawing of the model is presented in figure 2 and photographs of the model are presented in figure 3. The scaled-up mass and geometric characteristics of the model as compared with the estimated values for the full-scale configuration are given in table II.

For the flight tests, an electrically operated control system was installed in the model and ballast was added to locate the center of gravity (0.66 body length aft of nose and 0.19 body length below basic cone center line) properly. No attempt was made to simulate the estimated full-scale values of principal axis inclination or moments of inertia. (See table II.)

Although this configuration is not intended to be powered after reentry into the atmosphere, it was necessary to provide thrust for the purpose of conducting flight tests since gliding flight is not possible in the Langley full-scale tunnel. Thrust was provided by compressed air supplied through a flexible hose to a nozzle at the rear of the model alined with the model center of gravity. The amount of thrust could be varied and maximum output was about 60 pounds. The controls were operated by the pilots by means of proportional electric servomechanisms, but for some of the tests the gain was set to such a high value that essentially flicker-type control was used. The upper pair of control surfaces (hereafter called ailerons) were deflected differentially for roll and yaw control while the lower pair of control surfaces (hereafter called elevators) were deflected together for pitch control. The

undeflected or zero setting for all four control surfaces was taken as that position where the surface chord was parallel with the basic cone center line. For example, if the ailerons are alined with the top of the body, these surfaces would be considered deflected -6.6°; and if the elevators are alined tangent to the conical surface of the body, these surfaces would be considered deflected 30°. Aileron neutral position is defined as that trim setting of the upper surfaces about which these surfaces are deflected differentially for aileron control.

Static and dynamic force tests were conducted in the Langley free-flight tunnel by using the apparatus and testing technique described in reference 3. The flight investigation was conducted in the test section of the Langley full-scale tunnel with the test setup illustrated in figure 4. The flight-test equipment is described in detail in reference 4.

TESTS

Flight Tests

Flight tests were made to study the dynamic stability and control characteristics of the model for a center-of-gravity position of 0.66L over an angle-of-attack range from 15° to about 39°. Aileron deflections of about ±10° or less of each surface and elevator deflections of ±15° or less were used for all flight conditions. The model could not be tested at true scale weight because of tunnel limitations and hence the mass characteristics do not represent the full-scale vehicle. (See table II.)

The model behavior during the flight was observed by the pitch pilot located at the side of the test section and by the roll and yaw pilot located in the rear of the test section. The results obtained in the flight tests were primarily in the form of qualitative ratings of flight behavior based on pilot opinion. The motion-picture records obtained in the tests were used to verify and correlate the ratings for the different flight conditions.

Force Tests

In order to aid in the interpretation of the flight-test results, force tests were made to determine the static characteristics and dynamic stability derivatives of the flight-test model. All force tests were made at a dynamic pressure of 4.1 pounds per square foot which corresponds to an airspeed of about 60 feet per second at the standard

sea-level conditions and to a test Reynolds number of about 0.85×10^6 based on the body length of 2.22 feet.

The static longitudinal stability and control tests were made over an angle-of-attack range from 0° to 90° with elevator settings of 0°, 20°, and 40° for an aileron neutral position of -30° and also with both sets of control surfaces removed (body alone). Additional tests for longitudinal trim data were made over an angle-of-attack range from 0° to 40° with various settings of the elevator and the aileron neutral position.

The variation of the lateral coefficients with sideslip angle was measured over a β range from -15° to 15° for various angles of attack from 0° to 90° for the complete configuration. Since the variation of the lateral coefficients with β was approximately linear over the sideslip range tested throughout the entire angle-of-attack range, the static lateral stability derivatives for all configurations were determined from values of the lateral coefficients measured at $\pm5^\circ$ sideslip angle. The lateral control effectiveness was measured over an angle-of-attack range from 0° to 40° for various settings of the aileron neutral position.

Dynamic rolling and yawing oscillation tests to determine the rotary oscillation derivatives of the flight-test model were made over an angle-of-attack range from 0° to 90° with $\pm5^\circ$ amplitude in roll and yaw at frequencies of 0.4, 0.8, and 1.2 cycles per second which correspond to values of the reduced frequency parameter k of 0.07, 0.14, and 0.21, respectively. The rotary oscillation derivatives were also measured with the control surfaces undeflected and removed entirely ($k = 0.14$ only).

STABILITY AND CONTROL PARAMETERS OF FLIGHT-TEST MODEL

Static Longitudinal Stability and Control

The static longitudinal characteristics of the model over the angle-of-attack range from 0° to 90° for three elevator settings and for the body alone are presented in figure 5 (for aileron neutral position of -30° only). These data indicate that the longitudinal stability of the model is high throughout the angle-of-attack range and that the body alone is also stable for the center of gravity used in this investigation. The results also indicate that the elevator control surfaces maintained their effectiveness throughout the entire angle-of-attack range.

Since changes in longitudinal trim may result from moving the ailerons to neutral positions other than that presented for figure 5, data were obtained with a systematic variation of the elevator deflection for various aileron neutral settings. These results are presented in figure 6 for an angle-of-attack range from 0° to 40° and provide the means for a more detailed study of the longitudinal trim characteristics of the model than is possible with the data of figure 5. In general, the results indicate that the elevator surfaces provided trim to an angle of attack of about 29° although rather large control deflections were required. Maximum trimmed lift-drag ratios of the order of 1.0 were obtained. The summary plot of the pitching-moment characteristics presented as figure 6(f) indicates increasing stability as the aileron neutral position was moved upward. It should be noted, however, that the maximum trim angle of attack was not appreciably increased by moving the aileron neutral position upward.

The effects of the ailerons on trim and stability are perhaps more easily seen in figure 7 which shows the effects of using the ailerons as a pitch control for various settings of the elevators. (This plot is a cross plot of figure 6(f).) These effects may be explained as follows: the ailerons are effective pitch controls at the lower angles of attack, but these surfaces gradually lose their effectiveness with increasing angle of attack because they move into the low dynamic pressure region in the wake of the body. At the higher angles of attack ($\alpha > 30^\circ$) these surfaces contribute practically no pitching moment regardless of the amount of deflection; consequently, the maximum trim angle of attack was not appreciably changed by deflection of these surfaces. The increasing stability with upward deflection of these surfaces is, of course, a direct result of the positive effectiveness of these surfaces at the lower angles of attack and zero effectiveness at the higher angles of attack.

Since the flight cable was attached to the model directly above the center of gravity for the flight tests, and since the center of gravity was located deep in the body, an appreciable nose-up pitching moment was obtained as a result of drag on the flight cable. The data of figure 8 show the extent of the flight-cable influence on the longitudinal characteristics. An appreciable stabilizing effect due to the flight cable is indicated and the resulting nose-up pitching moment effectively increased by about 18° the elevator setting required for any given trim angle of attack. In addition to its effect on the pitching moments, the flight cable also added an increment to both lift and drag. In general, only minor differences are indicated for the L/D variations because of the compensating effects of the increments of lift and drag due to the flight cable.

It was suggested in reference 1 that all four control surfaces might be deflected outward and thus serve as drag brakes for controlling

the glide path of the vehicle after reentry. The effect of symmetrically deflecting outward the control surfaces on the longitudinal aerodynamic characteristics is illustrated in figure 9. The increased drag due to symmetrically deflecting the control surfaces proved effective in reducing the trim lift-drag ratio (see dashed curve on L/D plot) from a value of about 1.0 to about 0.6 while trim angle of attack is reduced from about 24° to 14°. It may be noted that some changes in longitudinal trim and increased static stability result from symmetrically deflecting the control surfaces.

Static Lateral Stability and Control

The static lateral stability data for the complete configuration (elevators down 30°; aileron neutral position up 10°) are presented in figure 10 as the variation of the coefficients C_Y, C_n, and C_l with angle of sideslip for various angles of attack from 0° to 90°. In general, the variation of the lateral coefficients with angle of sideslip was nearly linear over the angle-of-attack and sideslip ranges tested. These data, together with data for the configuration with the elevator removed (aileron neutral up 10°) and the configuration with all surfaces removed (body alone), are summarized in figure 11 as the variation with angle of attack of the side-force parameter C_{Y_β}, the directional stability parameter C_{n_β}, and the effective dihedral parameter C_{l_β}. These data indicate good directional stability and positive effective dihedral for the complete configuration over the entire angle-of-attack range (0° to 90°). The control surfaces had only a small effect on the directional stability and effective dihedral characteristics.

The lateral control characteristics of the model over the angle-of-attack range from 0° to 40° are shown in figure 12. These data are presented for various aileron neutral settings in terms of incremental lateral coefficients due to ±10° differential deflection of the upper pair of control surfaces (which correspond to approximately the maximum deflections used in the flight tests). With the aileron neutral position parallel to the basic cone center line the roll control effectiveness gradually decreased with increasing angle of attack and aileron reversal is indicated for angles of attack higher than 24°; the yawing moments due to aileron deflection were adverse for all angles of attack up to 40°. The control effectiveness was generally improved by movement of the surfaces upward out of the wake of the body but a decrease in roll-control effectiveness with increasing angle of attack is indicated for all aileron neutral positions; also, the yawing moments due to aileron deflection became favorable with upward movement of the aileron neutral position. With the aileron neutral setting of -40°, stalling

of the up-going surface caused reduced rolling and yawing effectiveness in the low angle-of-attack region.

Dynamic Oscillation Derivatives

Results obtained from rotary oscillation tests of the complete configuration with elevators down 20° and aileron neutral -30°, with all surfaces undeflected, and with the body alone (all surfaces removed) are presented in figures 13 to 16. In general, these data indicate that the complete configuration has damping in both roll and yaw throughout the angle-of-attack range (15° to 39°) covered in the flight tests. It should be noted, however, that for a slightly higher angle of attack (α between about 40° and 60°) negative damping in yaw is indicated (positive values for $C_{n_r} - C_{n_{\dot{\beta}}} \cos \alpha$). (See fig. 15.) Removal of the control surfaces, in general, reduced both the damping in roll and damping in yaw, but it may be noted that a large portion of both roll and yaw damping is produced by the body alone.

FLIGHT-TEST RESULTS AND DISCUSSION

A motion-picture film supplement covering the flight tests has been prepared and is available on loan. A request card form and a description of the film will be found at the back of this paper, on the page immediately preceding the abstract and index page. Table III provides descriptive remarks and numerical data corresponding to each of the flight tests shown in this film supplement. This table is intended primarily as an aid for interpreting the film, but it also serves as a convenient summary of results for the entire flight-test investigation.

Interpretation of Flight-Test Results

The primary purpose of these tests was to evaluate the dynamic stability and control characteristics of the proposed reentry configuration for the subsonic phase of the flight. The flight cable has been shown to produce a nose-up pitching moment of such magnitude that approximately 18° more down elevator deflection is required for a given trim angle of attack than would be needed in complete free flight. Since there was no loss in longitudinal control effectiveness with increasing elevator deflection (see fig. 6(f)) and since evaluation of the lateral control characteristics was made on the basis of upper surface neutral setting at various trim angles of attack, there should be no significant changes in either the longitudinal or lateral control characteristics due to the greater elevator deflection necessary to compensate for the

effect of the flight cable. In order to minimize the effects of thrust on trim, the thrust axis was directed through the model center of gravity.

Although the scale mass and inertia characteristics were not simulated in these tests, the scaled-up radii of gyration were of approximately the right magnitude. Inclination of the principal axis of inertia was only about $10°$ nose up compared with the full-scale value of $27°$ nose up. (See table II.) Since the moments of inertia, inclination of the principal axis, and glide-path angle can have appreciable effects on damping of the lateral oscillation (see ref. 5), a brief theoretical study for one flight condition was made to determine the effect of these discrepancies on the period and damping of the lateral motions and the results of this study are summarized in table IV. These calculations indicate that the flight-test results were somewhat optimistic because, if proper mass, moments of inertia, and inclination of the principal axis had been simulated in the tests, the periods of both the short- and long-period oscillations would have been considerably longer and the damping of these oscillations would not have been as good as was indicated by the model flight tests. (Compare first two columns of table IV.) Furthermore, if a gliding condition corresponding to a lift-drag ratio of about 1.0 had been simulated in the flight tests (see third column of table IV), the time for the Dutch roll oscillation to damp to half-amplitude would have been increased by a factor of about 1.5, although the period of this oscillation would have been about the same as for the level-flight case.

Longitudinal Stability and Control

The longitudinal stability characteristics of the model as determined from the flight tests were considered to be satisfactory for all flight conditions and were found generally to be independent of variations in aileron neutral position ($-10°$ to $-40°$), elevator position ($15°$ to $41°$), or angle of attack ($15°$ to $39°$). (See ratings of longitudinal stability characteristics in table III.) This longitudinal flight behavior reflects the large static margins (30 to 45 percent) shown in figures 5, 6, and 7.

The neutral setting of the ailerons, in conjunction with the positioning of the elevators, determined the longitudinal trim condition for each flight. The elevators provided a rather weak pitch control. More pitch maneuverability would have been desirable but, since no longitudinal trim or stability problem was encountered, very little pitch control was required and this deficiency presented no particular problem in these tests. (See table III.)

Lateral Stability and Control

The lateral stability characteristics of the model were considered to be satisfactory throughout the angle-of-attack range tested. The Dutch roll oscillation was well damped and appeared to be unaffected by changes in aileron neutral position, elevator position, or angle of attack over the range of these variables covered in the flight tests. (Refer to table III.)

The lateral control characteristics were largely dependent upon the neutral settings of the ailerons and the angle-of-attack range in which flights were attempted with a given aileron setting. It was impossible to fly the model for any angle of attack attempted with aileron neutral settings up to about -10° mainly because of the inadequate yaw control. (See fig. 12.) As the aileron neutral setting was moved upward, the lateral control characteristics improved (fig. 12) and sustained flights were possible up to an angle of attack of about 33°, depending on the neutral setting used. (See table III.) In the lower angle-of-attack range for conditions II, III, and IV (see table III), the model was easy to fly because response to control was very good. These control characteristics resulted in the model being easy to recover from very large disturbances. For each condition tested there was a gradual deterioration of the control characteristics as the angle of attack increased until a point was reached where sustained flights were impossible even with constant attention to control. At these angles of attack the model would fly smoothly until disturbed, and then it would sideslip back and forth across the test section several times until it finally went out of control against full opposite aileron. The inability to regain control after a disturbance within the confines of the test section does not necessarily indicate that recoveries would be impossible if more space were available as in free air.

Throughout the flight-test program the maximum angle of attack to which the model could be tested was limited by lateral control deficiency rather than by any lack of stability. Since all the flight characteristics, both longitudinal and lateral, were satisfactory throughout the test program with the exception of lateral control, the overall flight behavior rating of each flight condition was generally dependent on the corresponding lateral-control rating. (Refer to table III.)

CONCLUSIONS

The results of the investigation of the low-subsonic stability and control characteristics of a 1/3-scale free-flying model of a lifting-body reentry configuration may be summarized as follows:

CONFIDENTIAL

1. Longitudinal stability was satisfactory for all flight conditions tested, and although the elevators provided a rather weak pitch control, this deficiency presented no particular problem in these tests since there were no abrupt changes in trim or stability.

2. The lateral stability characteristics of the model were considered to be satisfactory throughout the angle-of-attack range tested. The Dutch roll oscillation was well damped and appeared to be unaffected by changes in aileron neutral position, elevator position, or angle of attack over the range of these variables covered in the flight tests.

3. The lateral control effectiveness decreased with increasing angle of attack and increased as the neutral setting of the ailerons was moved upward. Adequate lateral control could be obtained for angles of attack up to about 33° if the ailerons were initially trimmed about 40° up.

Langley Research Center,
    National Aeronautics and Space Administration,
        Langley Field, Va., March 28, 1960.

REFERENCES

1. Eggers, Alfred J., Jr., and Wong, Thomas J.: Re-entry and Recovery of Near-Earth Satellites, With Particular Attention to a Manned Vehicle. NASA MEMO 10-2-58A, 1958.

2. Savage, Howard F., and Tinling, Bruce E.: Subsonic Aerodynamic Characteristics of Several Blunt, Lifting, Atmospheric-Entry Shapes. NASA MEMO 12-24-58A, 1959.

3. Hewes, Donald E.: Low-Subsonic Measurements of the Static and Oscillatory Lateral Stability Derivatives of a Sweptback-Wing Airplane Configuration at Angles of Attack From -10° to 90°. NASA MEMO 5-20-59L, 1959.

4. Paulson, John W., and Shanks, Robert E.: Investigation of Low-Subsonic Flight Characteristics of a Model of a Flat-Bottom Hypersonic Boost-Glide Configuration Having a 78° Delta Wing. NASA TM X-201, 1959.

5. Sternfield, Leonard: Effect of Product of Inertia on Lateral Stability. NACA TN 1193, 1947.

TABLE II

MASS AND GEOMETRIC CHARACTERISTICS

	Model values scaled up	Full-scale design
Body length, L, ft	6.667	6.667
Body span, b, ft	10.000	10.000
Plan-form area $\left(S = 0.9L^2\right)$, sq ft	40.000	40.000
Weight, W, lb	1,161	4,000
Wing loading, W/S, lb/sq ft	29.025	100
Mass, m, slugs	36.06	124.22
Moments of inertia (body axes):		
I_X, slug-ft^2	244.8	770.0
I_Y, slug-ft^2	215.1	783.0
I_Z, slug-ft^2	375.3	878.0
I_{XZ}, slug-ft^2	-23.0	-134.0
Inclination of principal axis of inertia, ϵ, deg	-9°51'	-27°24'
Radii of gyration (body axes):		
k_X, ft	2.604	2.495
k_Y, ft	2.958	2.514
k_Z, ft	3.228	2.660

TABLE I

DERIVATIVES MEASURED IN OSCILLATORY TESTS

Derivatives	Rolling	Yawing
In phase	$C_{l_\beta} \sin \alpha - k^2 C_{l_{\dot{p}}}$ $C_{n_\beta} \sin \alpha - k^2 C_{n_{\dot{p}}}$ $C_{Y_\beta} \sin \alpha - k^2 C_{Y_{\dot{p}}}$	$C_{l_\beta} \cos \alpha + k^2 C_{l_{\dot{r}}}$ $C_{n_\beta} \cos \alpha + k^2 C_{n_{\dot{r}}}$ $C_{Y_\beta} \cos \alpha + k^2 C_{Y_{\dot{r}}}$
Out of phase	$C_{l_p} + C_{l_{\dot\beta}} \sin \alpha$ $C_{n_p} + C_{n_{\dot\beta}} \sin \alpha$ $C_{Y_p} + C_{Y_{\dot\beta}} \sin \alpha$	$C_{l_r} - C_{l_{\dot\beta}} \cos \alpha$ $C_{n_r} - C_{n_{\dot\beta}} \cos \alpha$ $C_{Y_r} - C_{Y_{\dot\beta}} \cos \alpha$

TABLE III.- SUMMARY OF MODEL FLIGHT BEHAVIOR

Flight condition number	Film supplement scene number	Aileron neutral position[1], deg	Elevator neutral position[2], deg	Angle of attack, α, deg	Tunnel velocity, V, ft/sec	Longitudinal stability characteristics	Longitudinal control characteristics	Lateral stability characteristics	Lateral control characteristics	Overall flight behavior rating
I-a		-10	26	22	74	Very good	Adequate[3]	Not determined.	Inadequate[4]	Unflyable because of inadequate lateral control
II-a	1	-20	41	15	85	Very good	Adequate	Very good; Dutch roll well damped.	Good- recoveries from rough air disturbances possible sometimes.	Fair- rough air stream caused main flight difficulty.[5]
II-b		-20	30	18	81	Very good	Adequate	Very good.	Good- recoveries from moderate disturbances possible.	Good- very smooth flight condition.
II-c		-20	25	22	77	Very good	Adequate	Very good.	Fairly good- but weaker than desired.	Fair- lateral control not as powerful as desired.
II-d	2	-20	21	26	74	Very good	Adequate	Very good.	Weak- especially after disturbance.	Poor- because of weak lateral control.
II-e	3	-20	18	31	68	Not determined[6]	Not determined[6]	Not determined[6]	Inadequate[4]	Sustained flight impossible- because of inadequate lateral control.[7]
III-a		-30	38	18	61	Very good	Adequate	Very good; dead beat Dutch roll damping	Good- some tendency to over-control.[8]	Good
III-b		-30	33	21	77	Very good	Adequate	Very good.	Very good- recoveries from large disturbances were possible.	Very good
III-c		-30	28	26	74	Very good	Adequate	Very good.	Very good	Very good- one of best conditions tested.
III-d	4	-30	25	30	68	Very good	Adequate	Very good.	Weak- especially after disturbance.	Poor- because of weak lateral control.
III-e		-30	23	34	62	Very good	Adequate	Good[9]; no oscillation observed.	Inadequate[4]	Good when undisturbed but sustained flight impossible after disturbance because of inadequate lateral control.[7]
IV-a	5	-40	19	33	62	Very good	Adequate	Very good; oscillation well damped.	Very good- much better than III-e at same α.	Very good- equal to III-c; much better than III-e at same α.
IV-b		-40	15	39	54	Very good	Adequate	Not determined[6]	Inadequate[4]	Poor- sustained flight impossible due to inadequate lateral control.[7]

1 Neutral setting of upper pair of control surfaces with respect to basic cone center line, negative values indicate trailing edges up.
2 Neutral setting of lower pair of control surfaces with respect to basic cone center line, positive values indicate trailing edges down.
3 Model flies itself longitudinally. More pitch maneuverability would be desirable, but since no longitudinal trim or stability problem was encountered control was rated adequate.
4 Model could not be banked to recover from a disturbance, so control was rated inadequate.
5 Rough air condition encountered at this tunnel velocity made direct comparison of model flight characteristics with other tests impossible.
6 Lateral divergence occurred before flight characteristics could be rated. Divergence probably due to inadequate lateral control.
7 Recoveries and sustained flight might be possible if more space were available as in free air.
8 Some tendency to over-control with aileron deflections used, but with reduced aileron travel this tendency could have been eliminated.
9 Directional stability is good. Model flies smoothly so long as it is not disturbed laterally.

CONFIDENTIAL

TABLE IV

CALCULATED LATERAL MOTION PERIOD AND TIME

TO DAMP TO HALF-AMPLITUDE

$\left[\alpha = 33^\circ; \; C_L = 1.17; \; \text{sea level; corresponds to scene number 5 of film supplement, table III}\right]$

	Model values scaled up	Full-scale design (estimated)	
	Level flight	Level flight	Gliding flight
γ, deg	0	0	-46°28'
μ_b	37.938	130.597	130.597
I_X, slug-ft^2	244.8	770.0	770.0
I_Z, slug-ft^2	375.3	878.0	878.0
I_{XZ}, slug-ft^2	-23.0	-134.5	-134.5
ϵ, deg	-9°51'	-27°24'	-27°24'
P (short-period oscillation), sec	3.462	5.997	5.758
$T_{1/2}$ (short-period oscillation), sec	3.095	6.199	9.090
$C_{1/2}$ (short-period oscillation), cycles	0.894	1.034	1.579
P (long-period oscillation), sec	20.707	45.056	15.875
$T_{1/2}$ (long-period oscillation), sec	3.045	15.043	8.487
$C_{1/2}$ (long-period oscillation), cycles	0.147	0.334	0.535
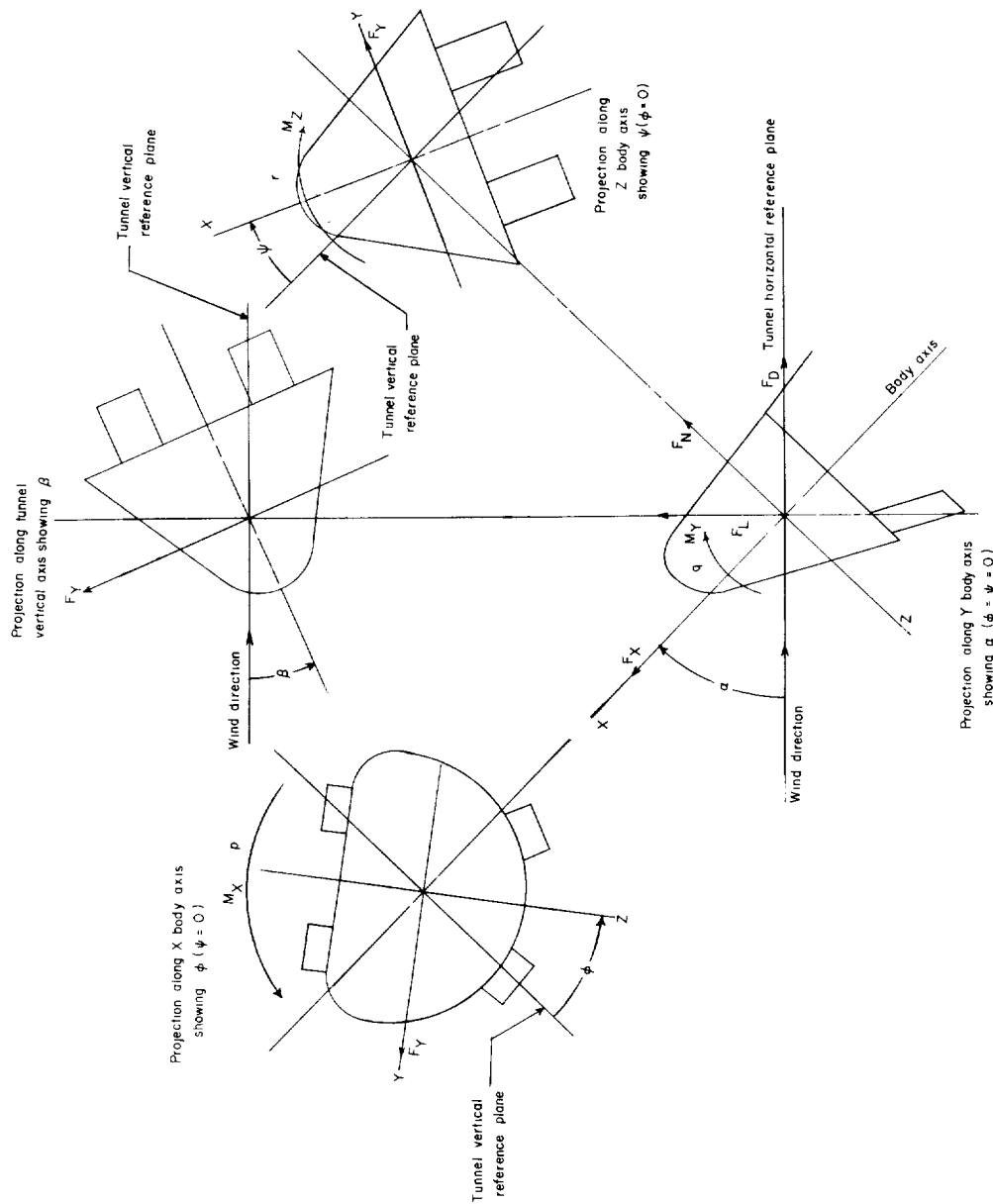
Figure 1.- System of axes used in investigation. Longitudinal data are referred to wind axes, and lateral data are referred to body axes. Arrows indicate positive directions of moments, forces, angular velocities, and angles.
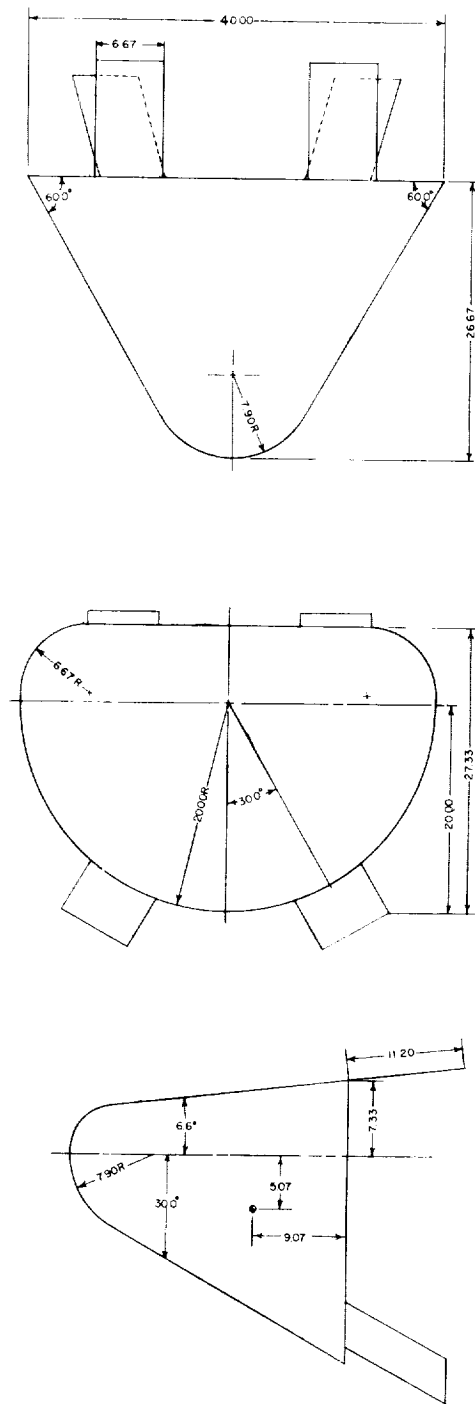
Figure 2.- Three-view drawing of 1/3-scale model used in investigation.
All linear dimensions are in inches.

(a) Model being prepared for flight test.   L-59-1540

Figure 3.- Photographs of 1/3-scale model used in investigation.

L-59-1542

(b) Model being flight tested in Langley full-scale tunnel test section.

Figure 3.- Concluded.
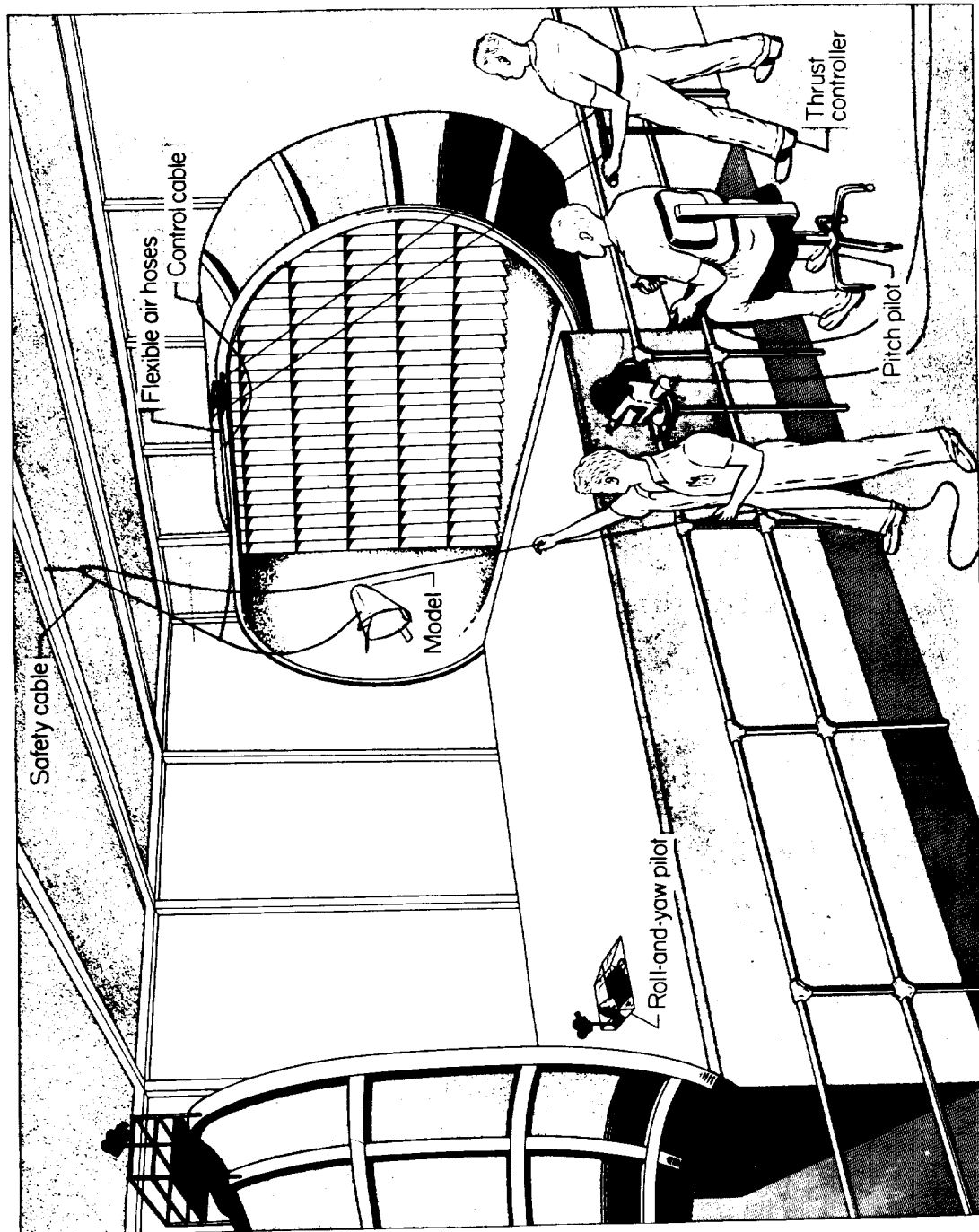
Figure 4.- Sketch of test setup in Langley full-scale tunnel.
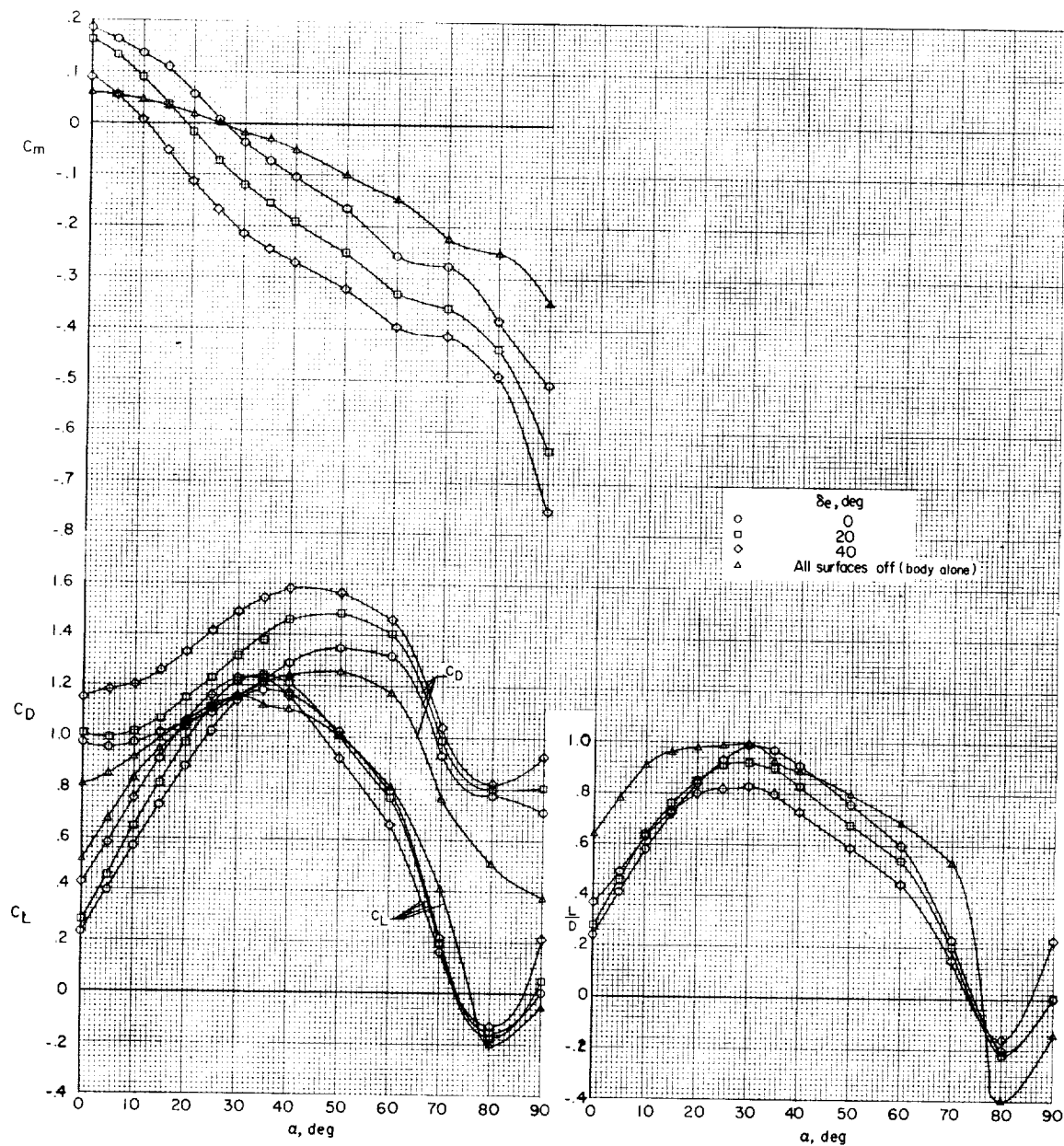
Figure 5.- Static longitudinal characteristics of the 1/3-scale flight-test model. Aileron neutral position, -30°; β = 0°.

	δ_e , deg
○	0
□	10
◇	20
△	30
◁	40
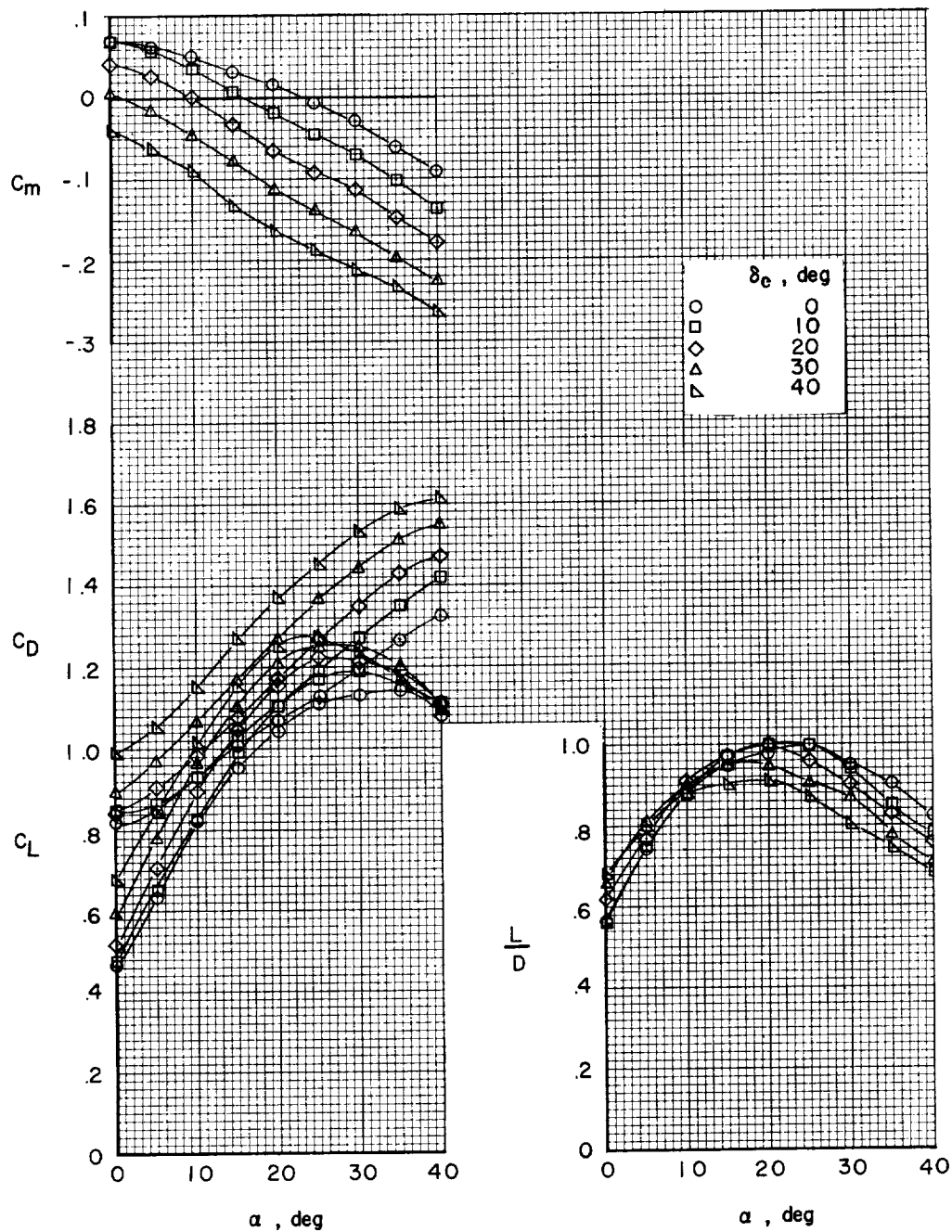
(a) Aileron neutral position, 0°.

Figure 6.- Effect of elevator deflection at various aileron neutral positions on longitudinal trim. β = 0°.
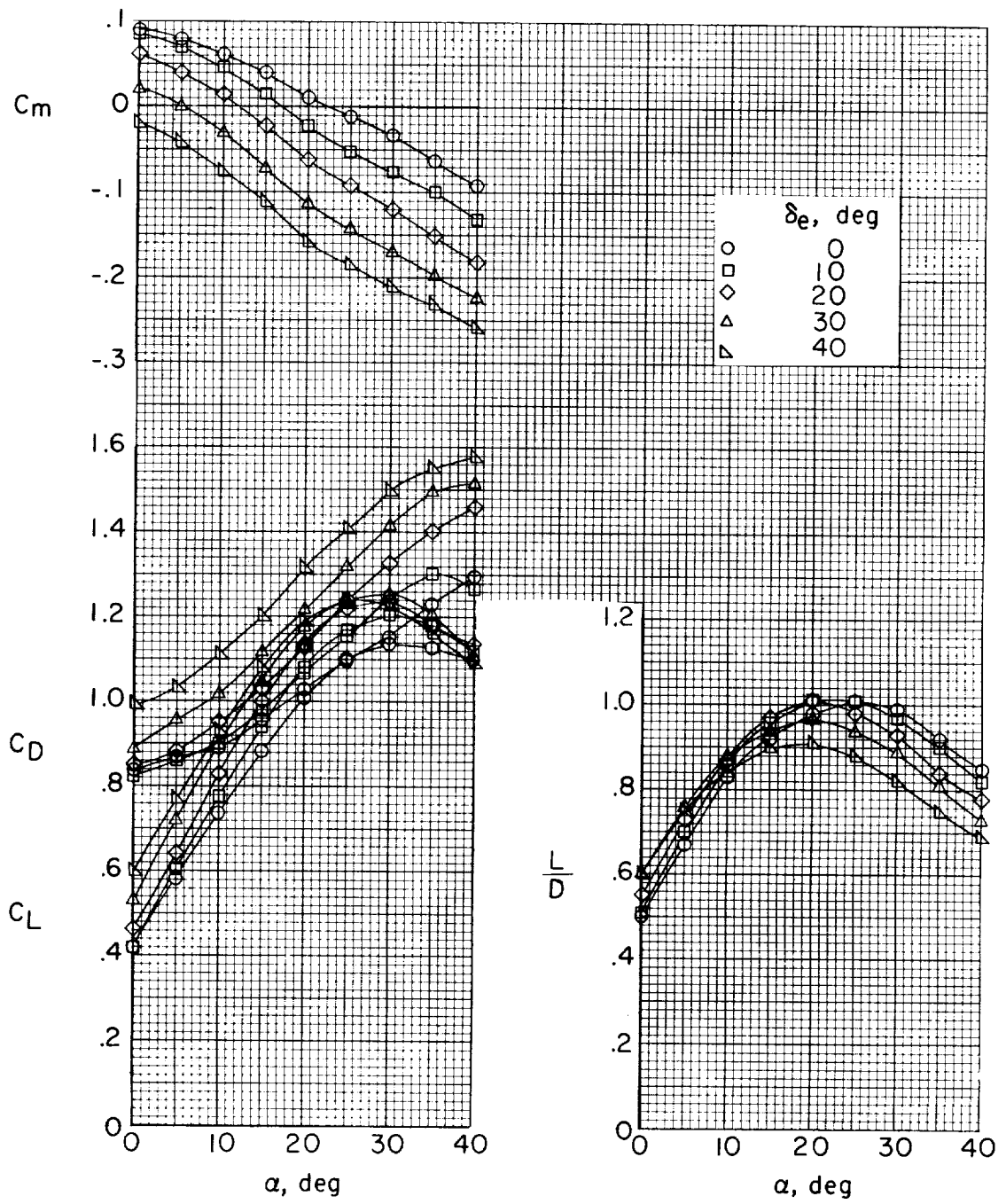
(b) Aileron neutral position, -10°.

Figure 6.- Continued.
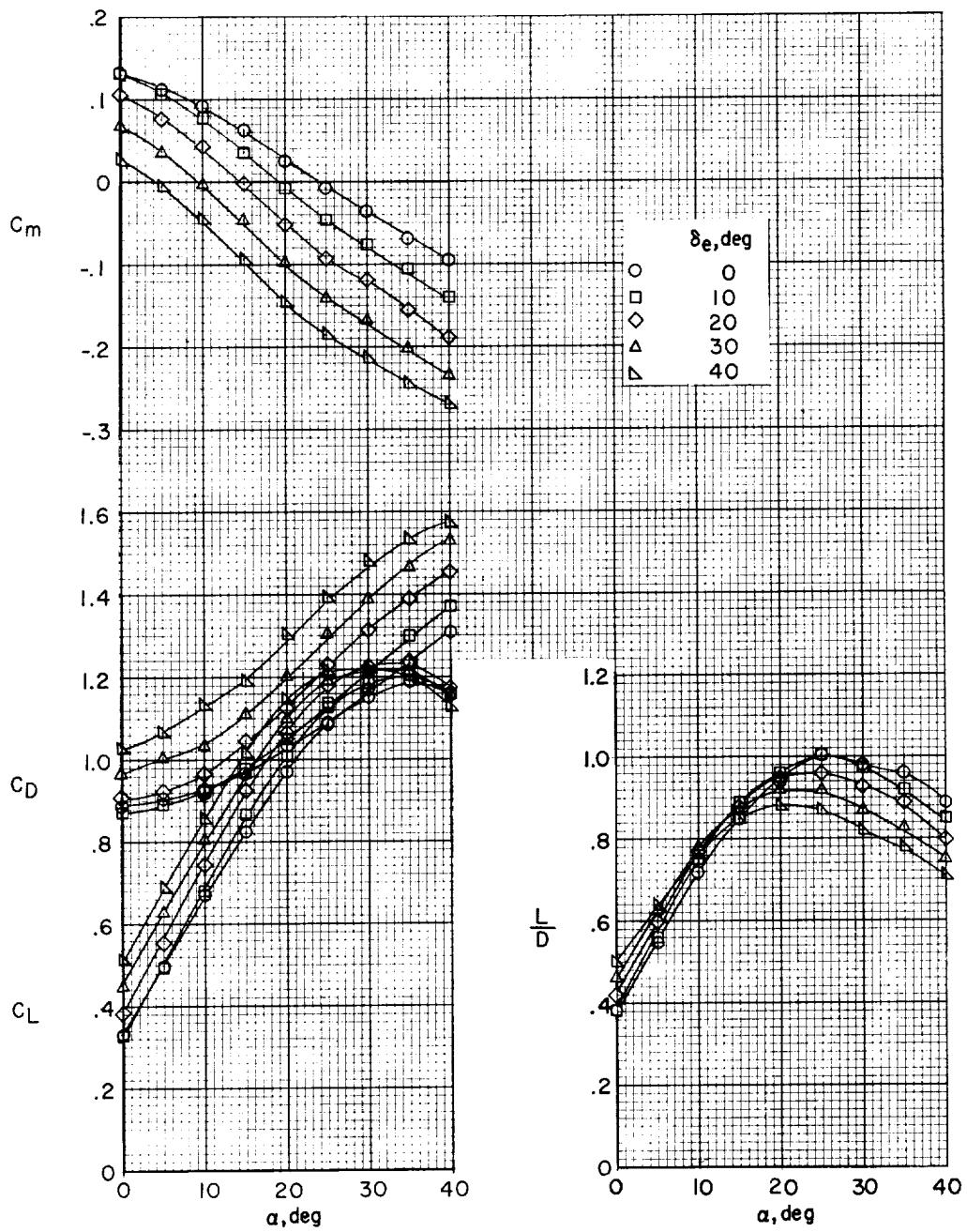
(c) Aileron neutral position, -20°.

Figure 6.- Continued.
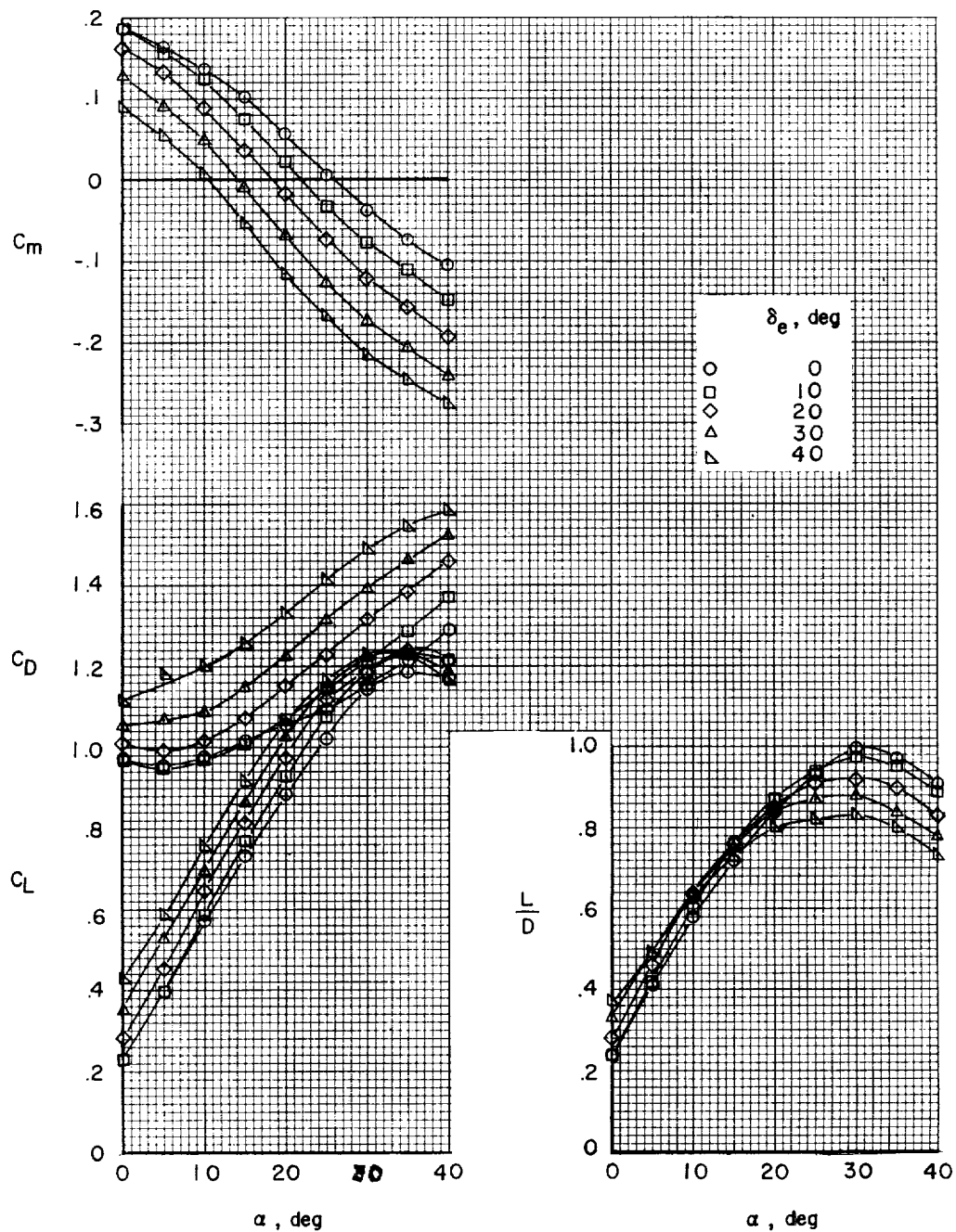
(d) Aileron neutral position, -30°.

Figure 6.- Continued.
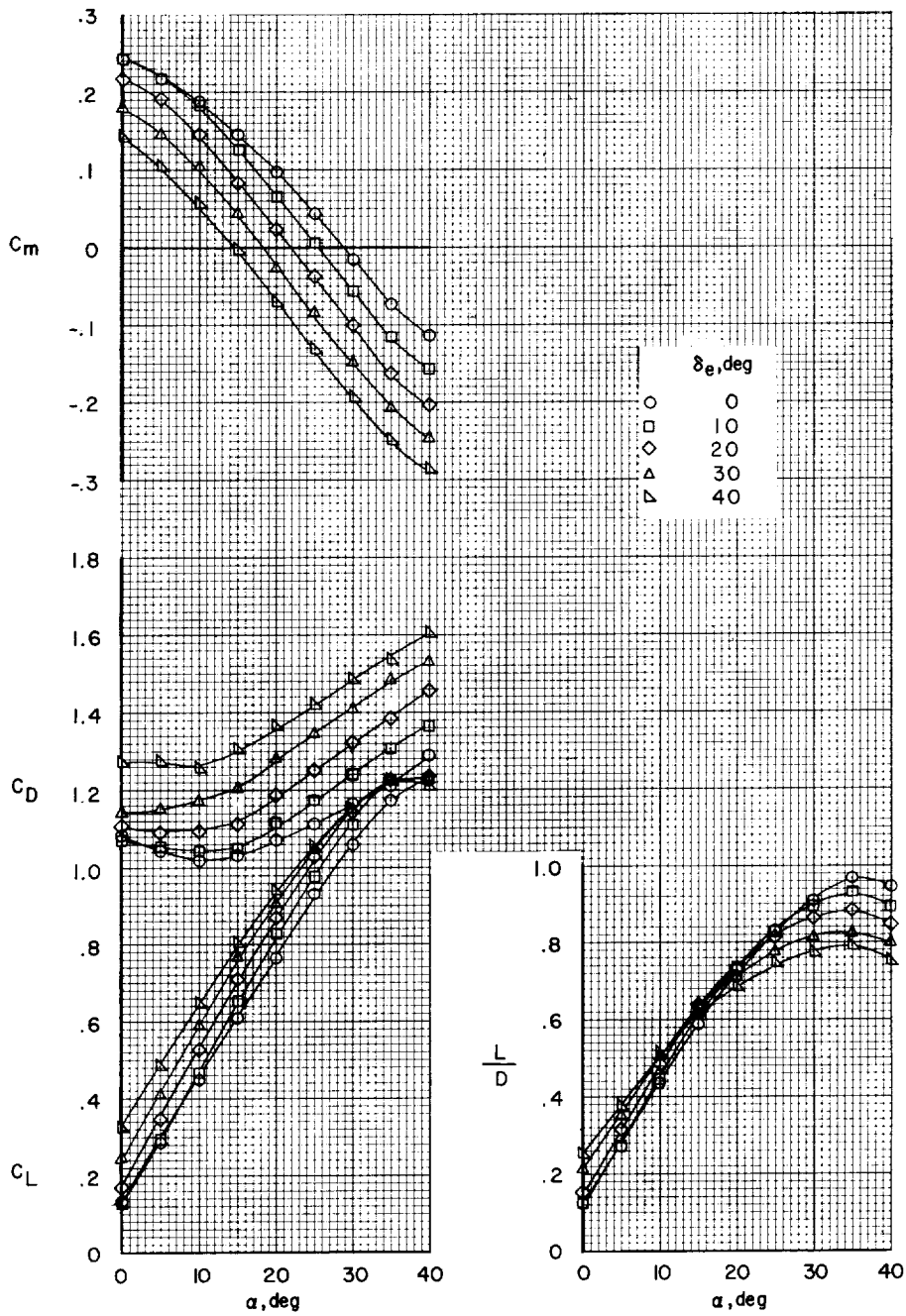
(e) Aileron neutral position, -40°.

Figure 6.- Continued.
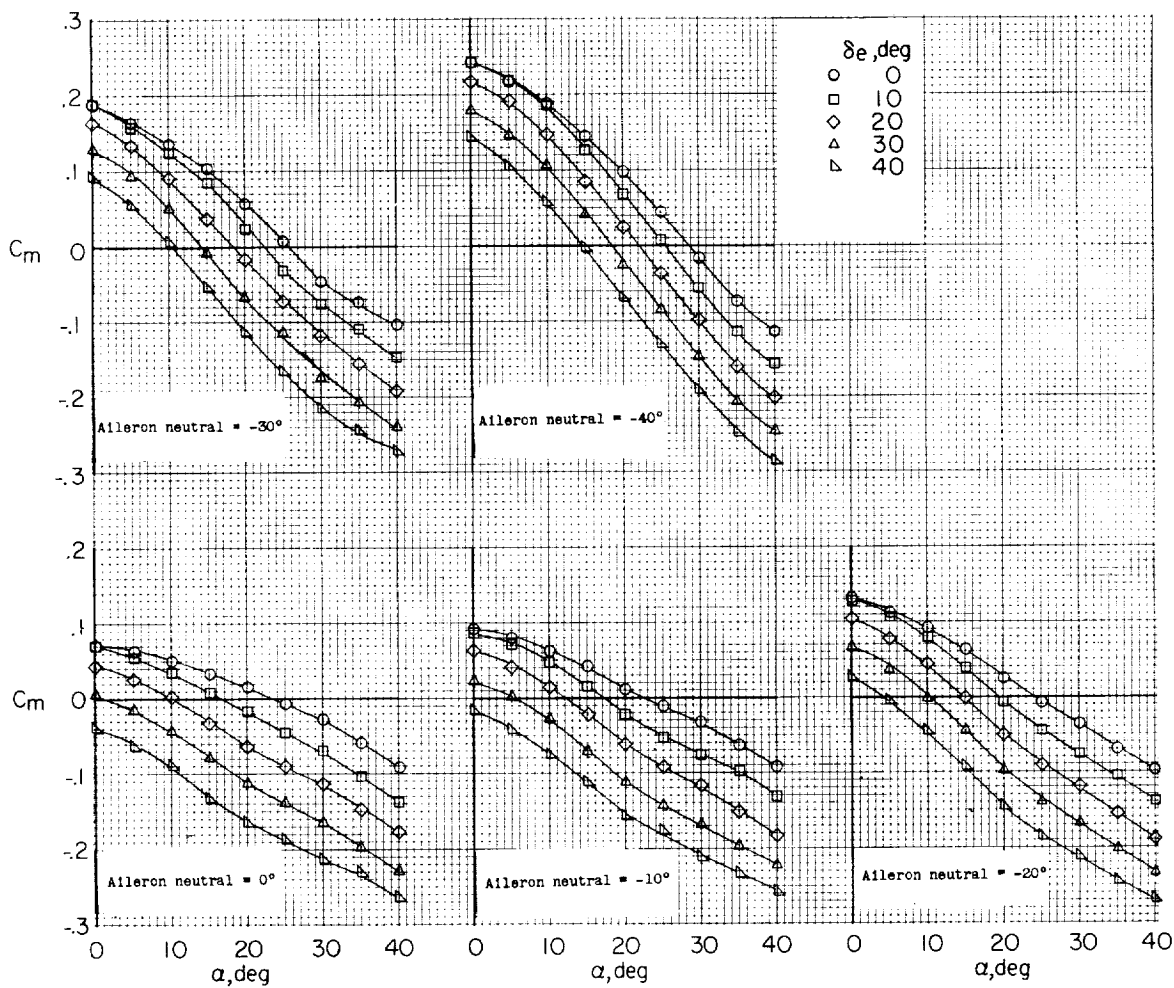
(f) Summary of variation of C_m with α.

Figure 6.- Concluded.
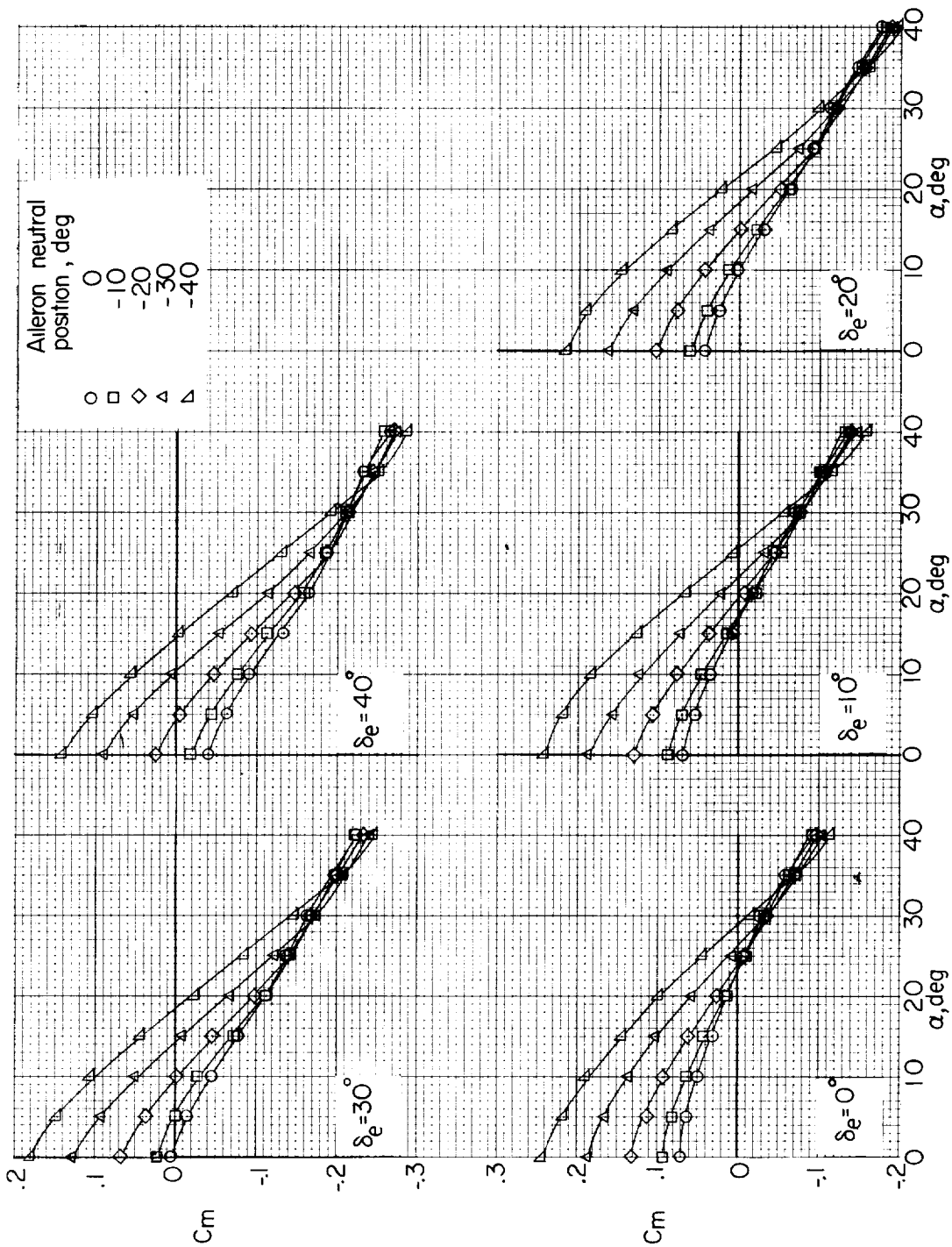
Figure 7.- Effect of using the ailerons as a pitch control.
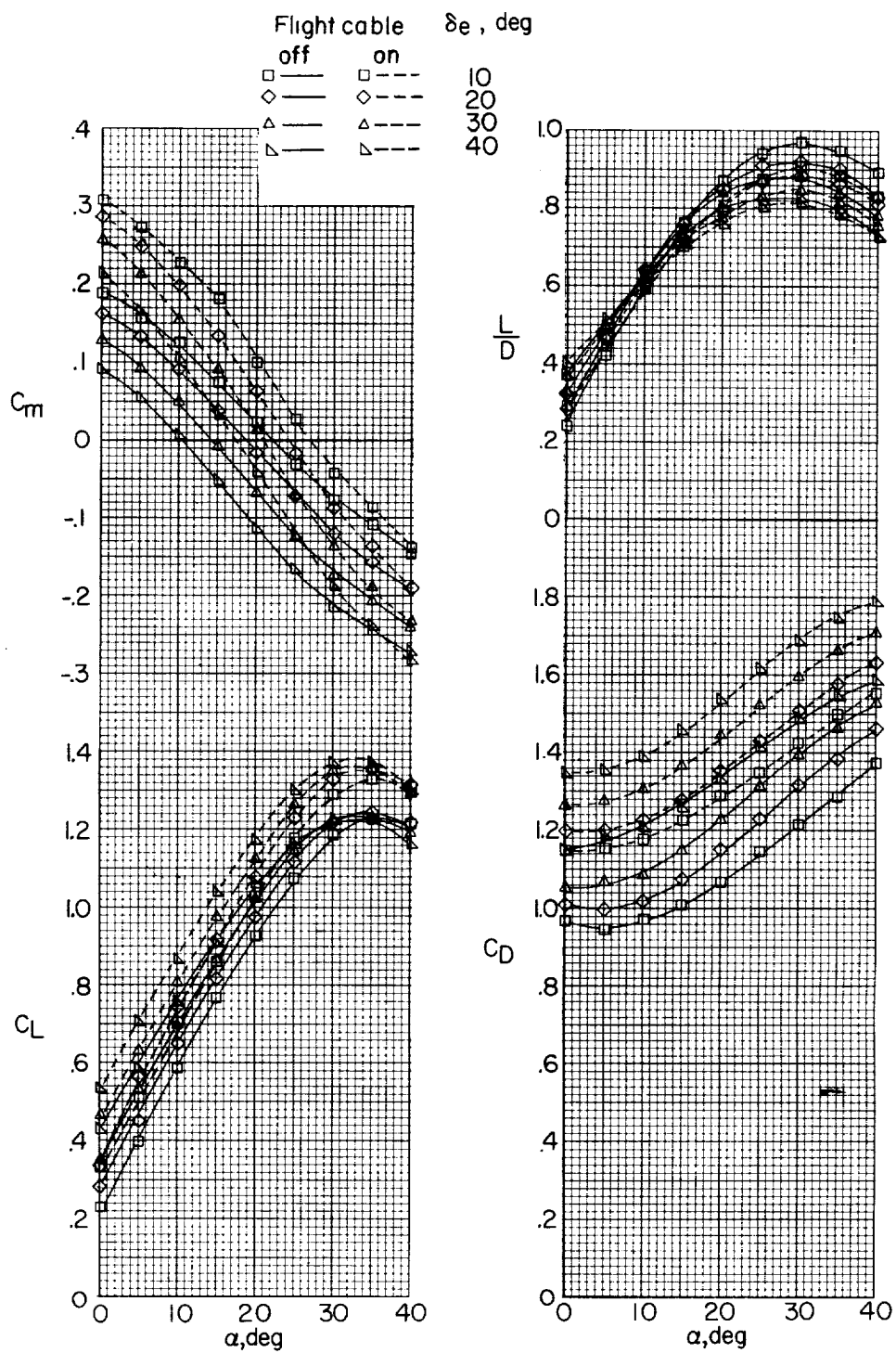
Figure 8.- Effect of model flight cable on longitudinal trim. Aileron neutral, -30°; β = 0°.
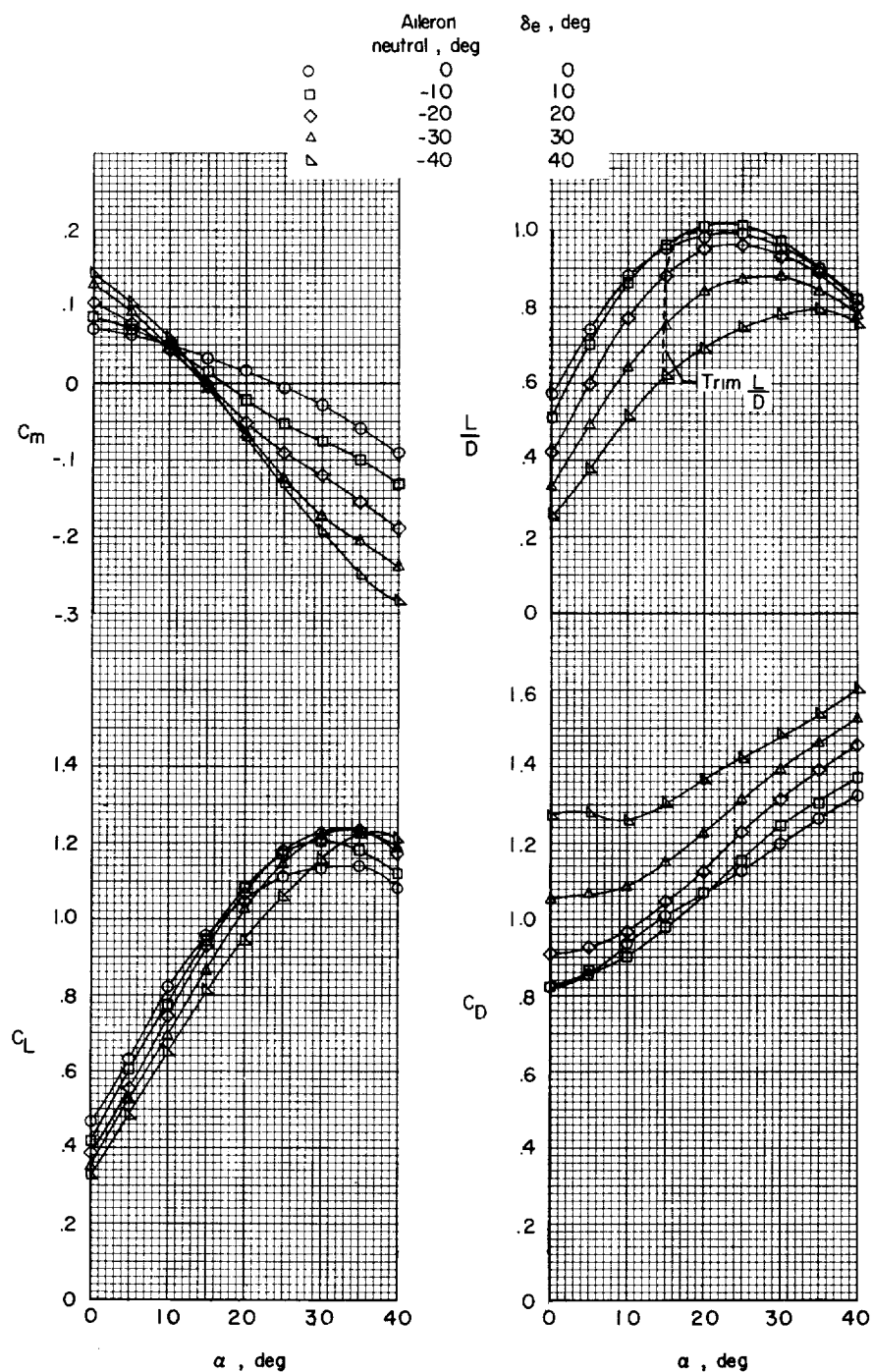
Figure 9.- Effect of symmetrically deflecting outward (for flight-path control) on static longitudinal aerodynamic characteristics. $\beta = 0^{\circ}$.
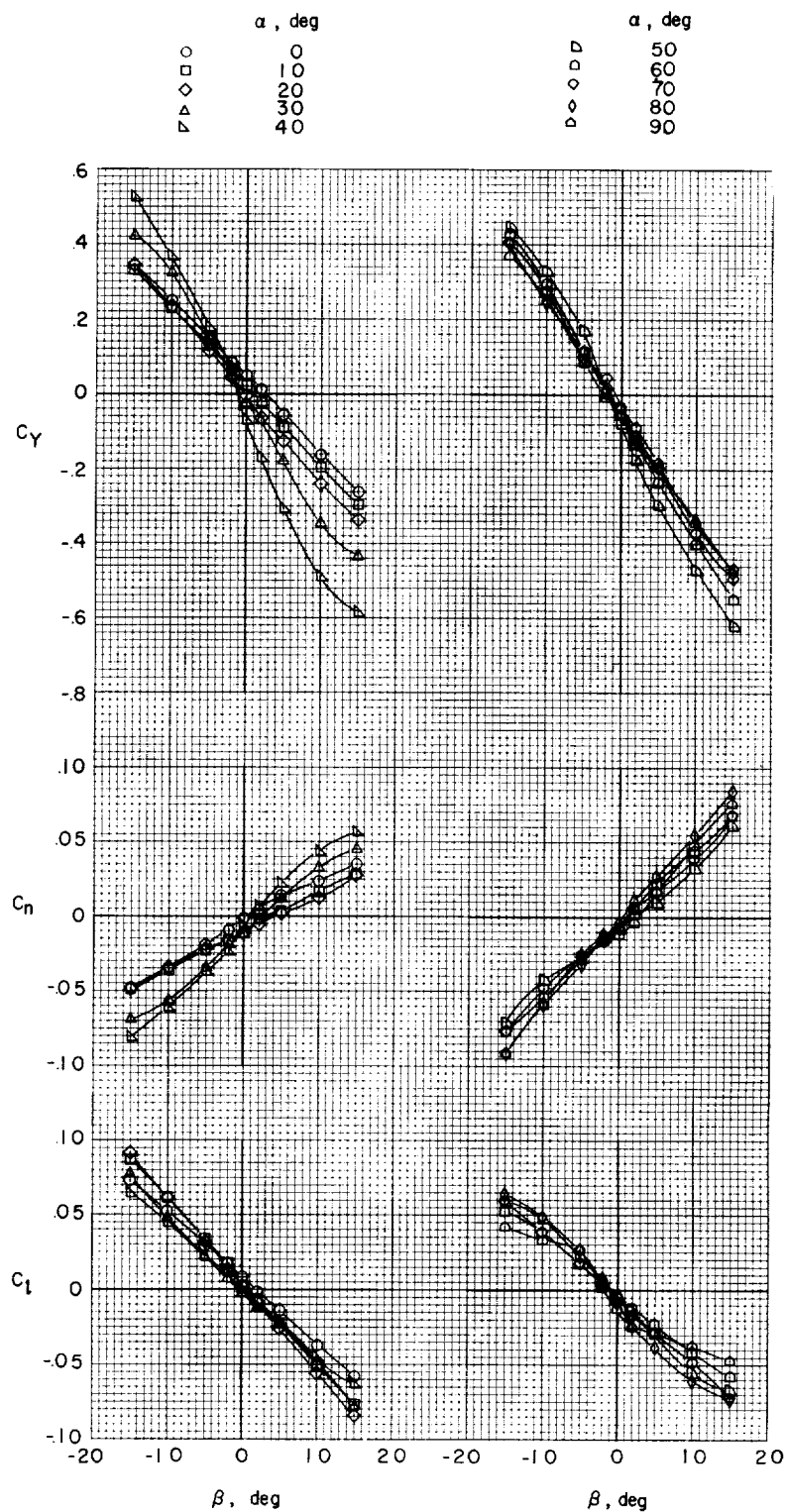
Figure 10.- Variation of static lateral coefficients with sideslip angle for the 1/3-scale flight-test model. Aileron neutral, -10°; $\delta_e = 30°$.

	Aileron neutral , deg	δ_e , deg
————————	-10	30
— — — — —	-10	Off
- - - - - - - - - - -	Off	Off
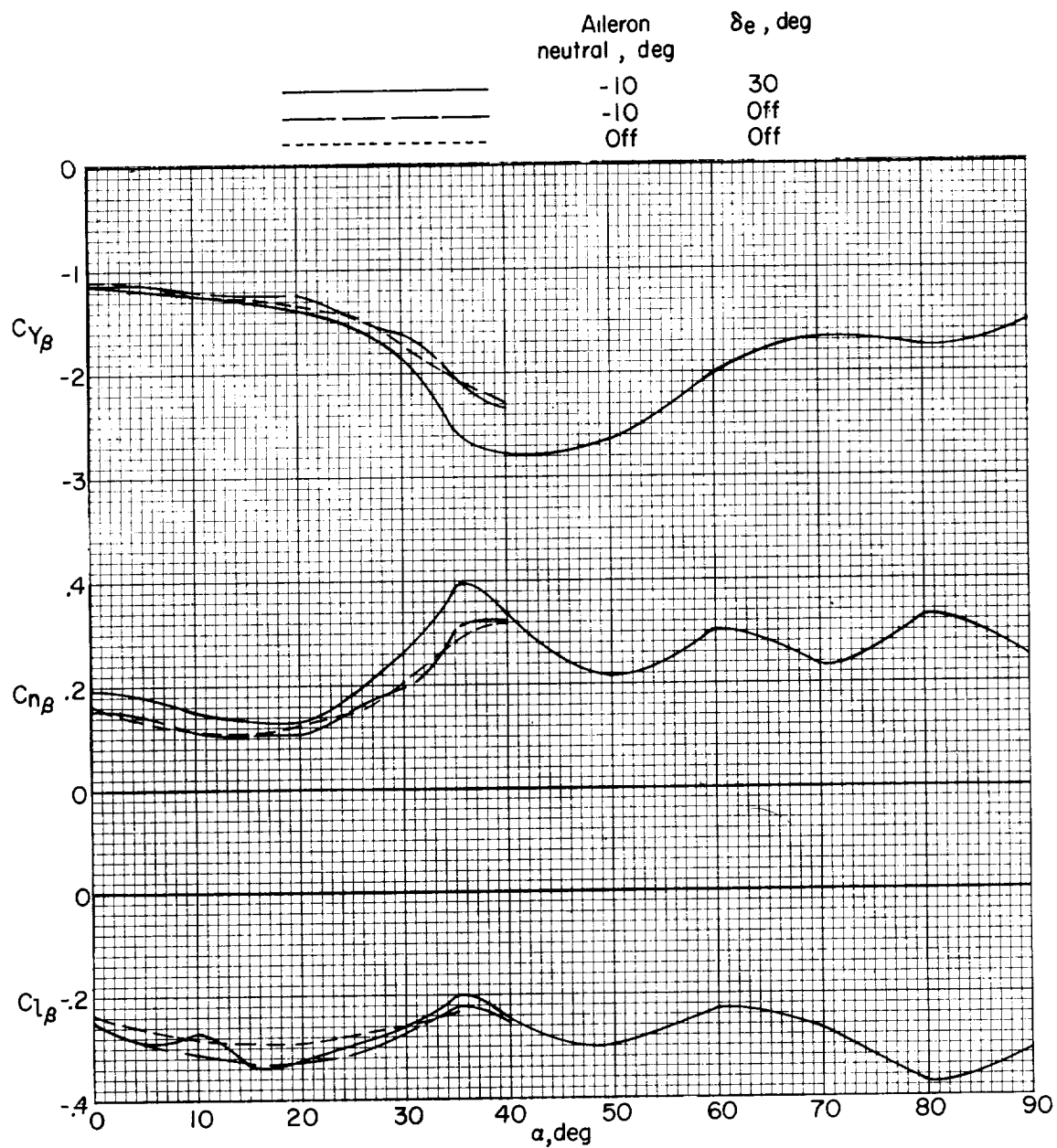
Figure 11.- Static lateral stability derivatives of 1/3-scale flight-test model.
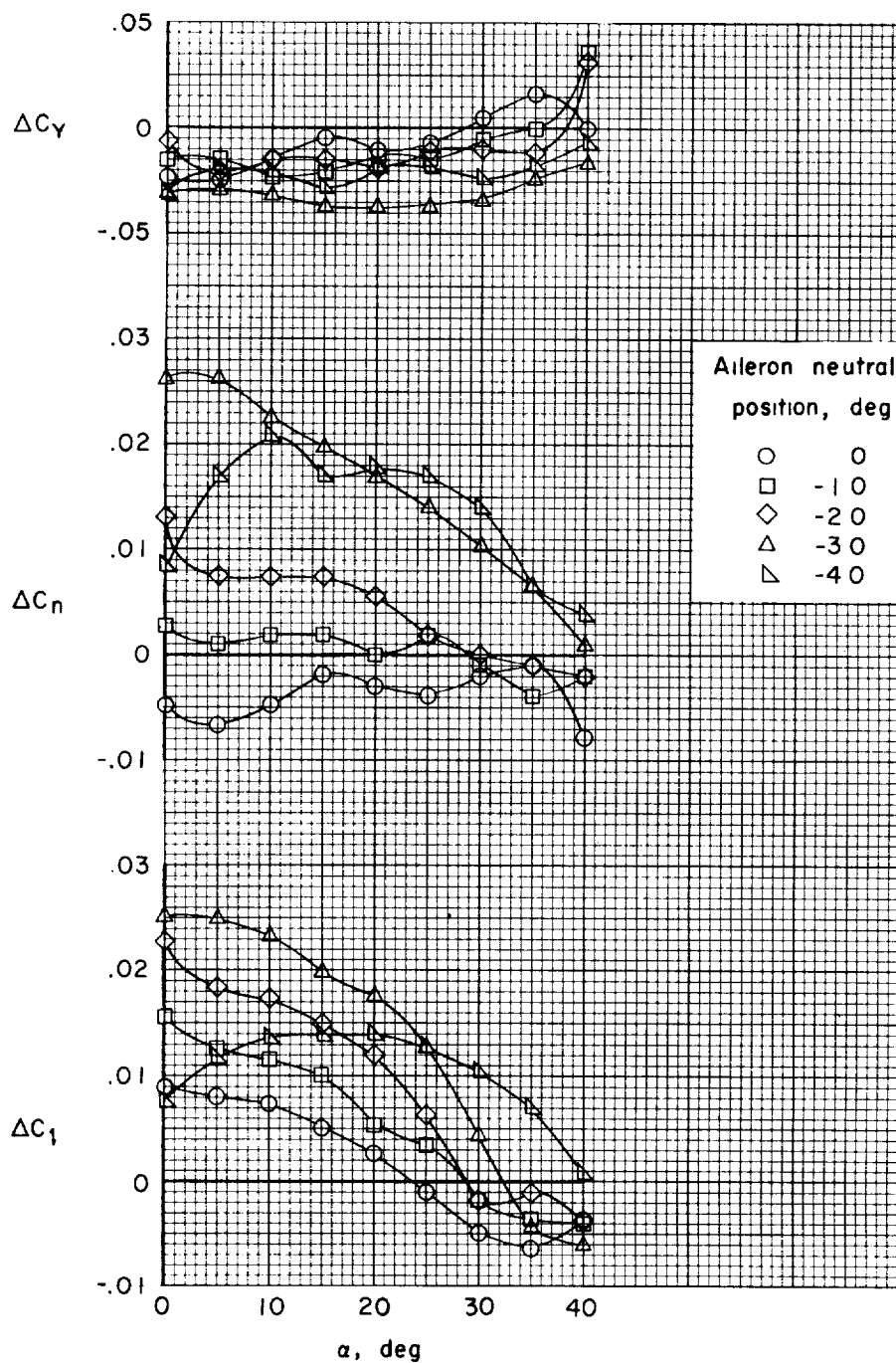
Figure 12.- Effect of aileron neutral position on increments in lateral force and moment coefficients produced by $\pm 10°$ differential deflection of the ailerons ($20°$ total control surface deflection). $\beta = 0°$.
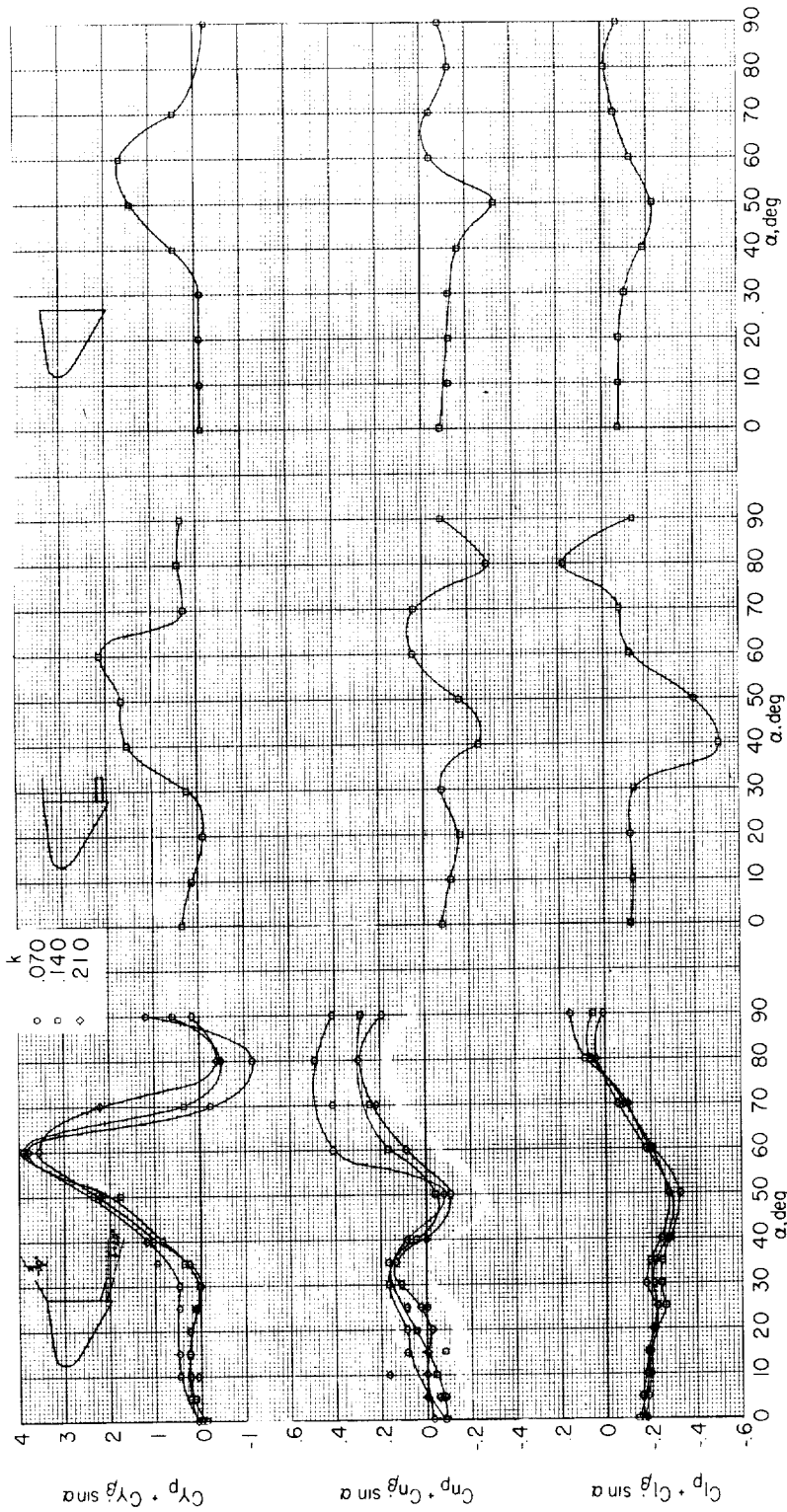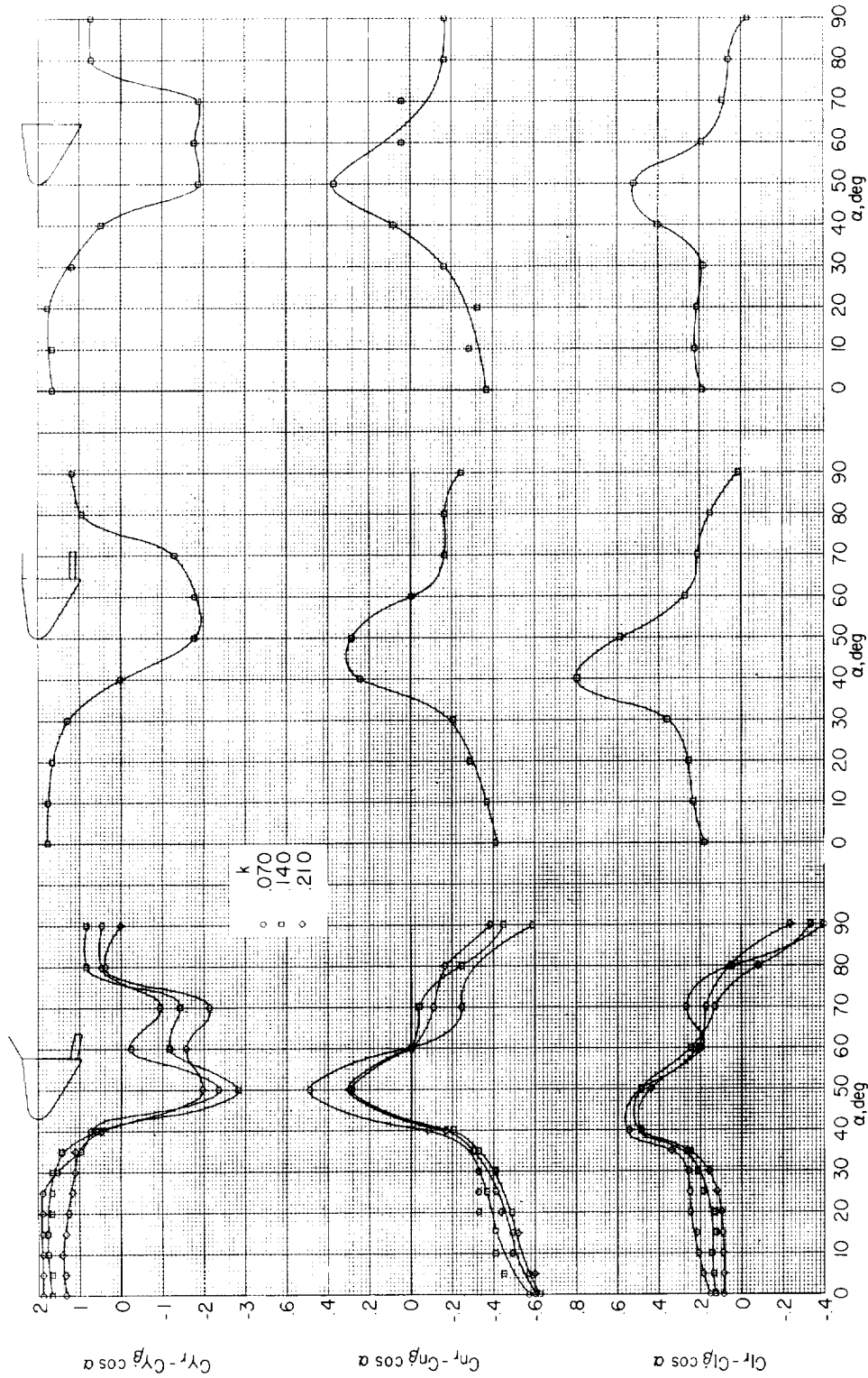
(a) Complete configuration.   (b) Complete configuration.   (c) All control surfaces off.
Aileron neutral, -30°;   All surfaces undeflected.
δ_e = 20°.

Figure 13.- Out-of-phase rolling derivatives of 1/3-scale flight-test model.
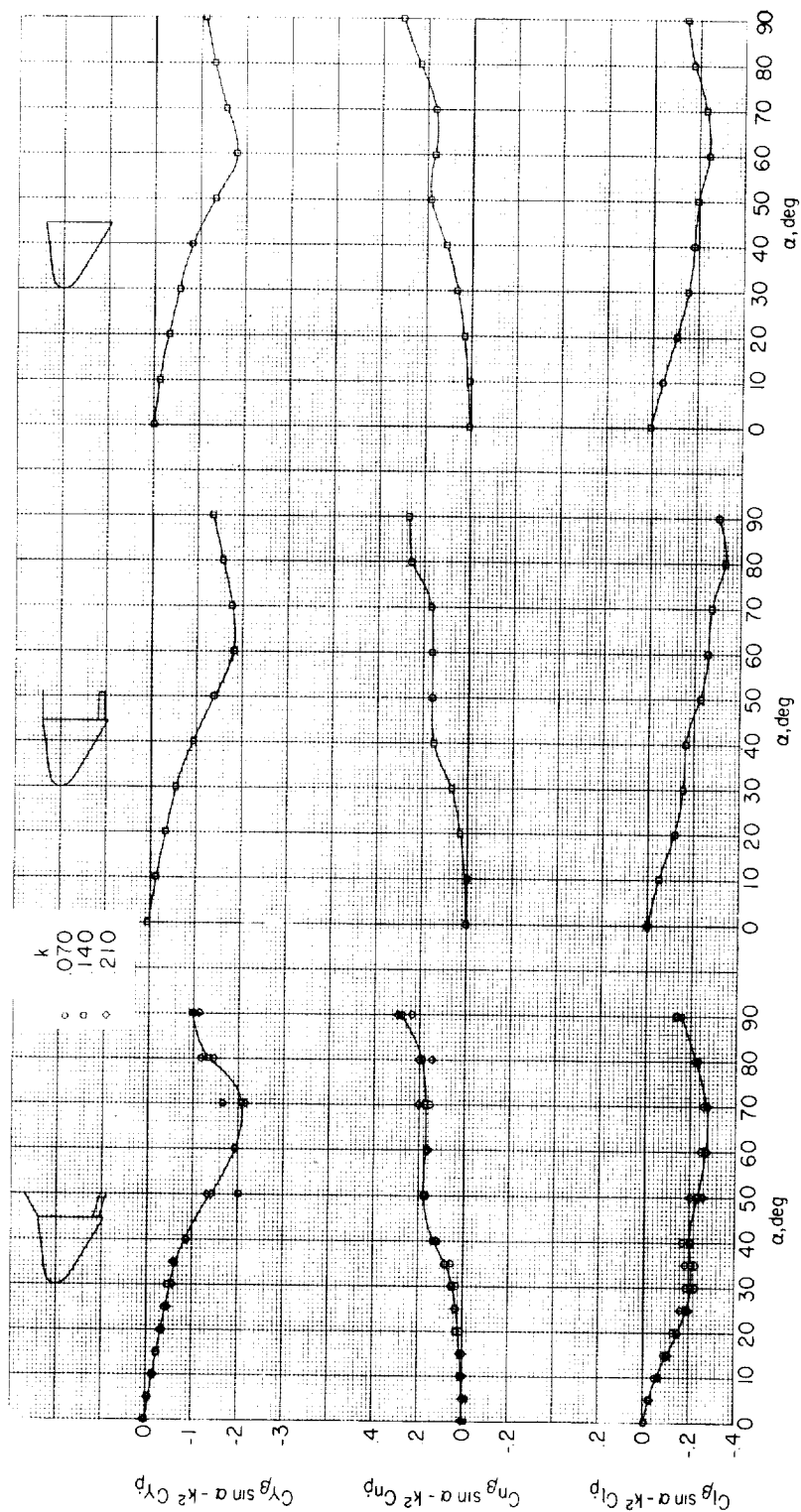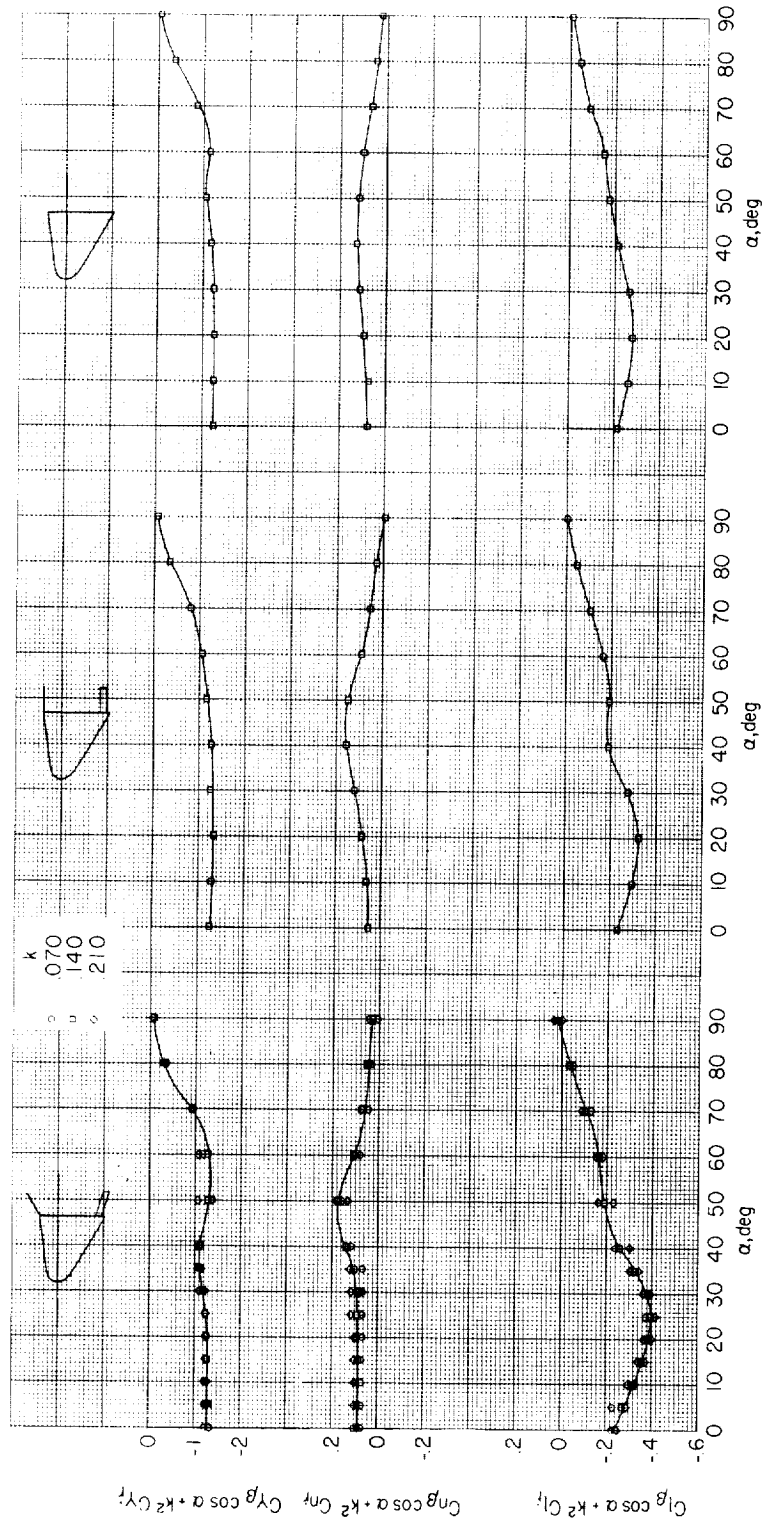
(a) Complete configuration.
Aileron neutral, -30°;
$\delta_e = 20°$.

(b) Complete configuration.
All surfaces undeflected.

(c) All control surfaces off.

Figure 14.- In-phase rolling derivatives of 1/3-scale flight-test model.

Figure 15.- Out-of-phase yawing derivatives of 1/3-scale flight-test model.

(a) Complete configuration.   (b) Complete configuration.   (c) All control surfaces off.
   Aileron neutral, -30°;   All surfaces undeflected.
   $\delta_e = 20°$.

(a) Complete configuration.
Aileron neutral, -30°;
$\delta_e = 20°$.

(b) Complete configuration.
All surfaces undeflected.

(c) All control surfaces off.

Figure 16.- In-phase yawing derivatives of 1/3-scale flight-test model.

A motion-picture film supplement, carrying the same classification of the report, is available on loan. Requests will be filled in the order received. You will be notified of the approximate date scheduled.

The film (16 mm, 12 min., B&W, silent) deals with the low-speed stability and control characteristics of a 1/3-scale free-flying model of a lifting-body reentry configuration.

Requests for the film should be addressed to the

    Technical Information Division
    Code BIV
    National Aeronautics and Space Administration
    Washington 25, D.C.

NOTE: The handling of requests for this classified film will be expedited if application for the loan is made by the individual to whom this copy of the report was issued. In line with established policy, classified material is sent only to previously designated individuals. Your cooperation in this regard will be appreciated.

CUT

Date————————

Please send, on loan, copy of film supplement to NASA
Technical Memorandum X-297 (Film L-537)

_____
Name of organization
_____
Street number
_____
City and State
Attention:*Mr.—————————————————————

        Title—————————————————————

        (*To whom copy No. ____ of the Technical Memorandum
                was issued)

Technical Information Division
Code BIV
National Aeronautics and Space Administration
Washington 25, D.C.